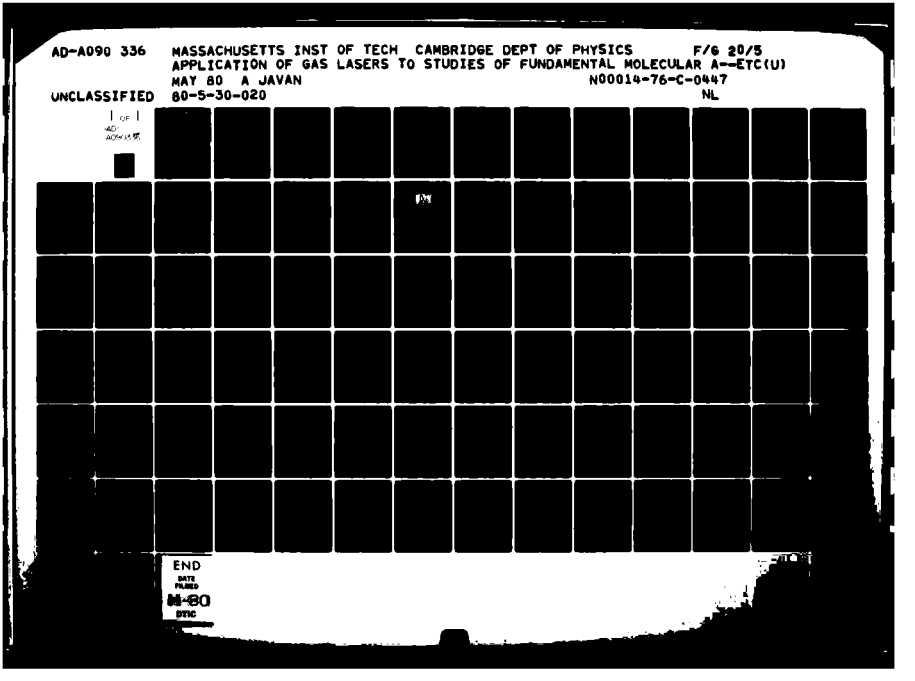
AD-A090 336
MASSACHUSETTS INST OF TECH CAMBRIDGE DEPT OF PHYSICS F/G 20/5
APPLICATION OF GAS LASERS TO STUDIES OF FUNDAMENTAL MOLECULAR A--ETC(U)
MAY 80 A JAVAN N00014-76-C-0447
UNCLASSIFIED 80-5-30-020 NL
1 OF 1
END
DATE FILMED
8-80
DTIC

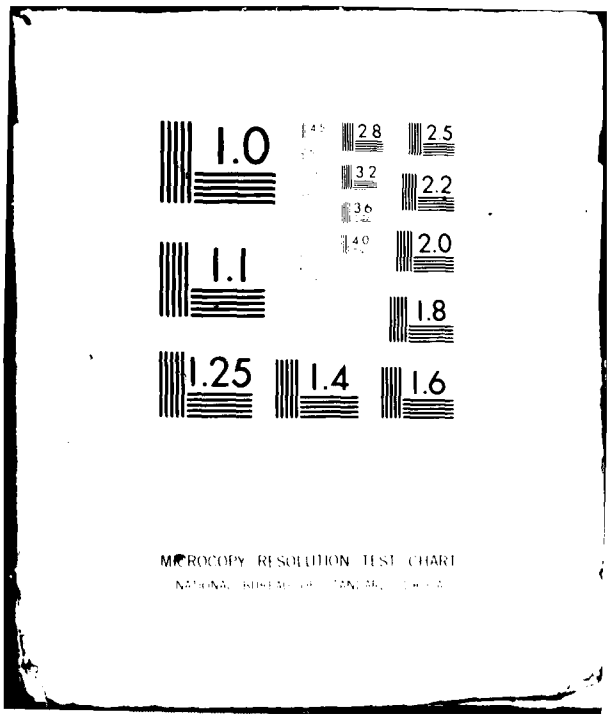
1.0
1.1
1.25
1.4
1.6
1.8
2.0
2.2
2.5
2.8
3.2
3.6
4.0
MICROCOPY RESOLUTION TEST CHART

12 May 1980

Massachusetts Institute of Technology

Cambridge, Massachusetts 02139

Department of Physics

Application of Gas Lasers to Studies of Fundamental Molecular and Atomic Processes

Final ~~Report~~

~~Covering the Period~~

1 July 1975 ~~through~~ 15 November 1979

Under Direction of ~~Professor~~ Ali Javan

Sponsored by:

Office of Naval Research

Attention: Dr. William J. Condell, Jr.

Contract Number: N00014-76-C-0447

Task: NR 395-504

M.I.T. Project 83259

UNCLASSIFIED

SECURITY CLASSIFICATION OF THIS PAGE (When Data Entered)

REPORT DOCUMENTATION PAGE		READ INSTRUCTIONS BEFORE COMPLETING FORM
1. REPORT NUMBER 80 5 30 020	2. GOVT ACCESSION NO. AD-A090 552	3. RECIPIENT'S CATALOG NUMBER
4. TITLE (and Subtitle) APPLICATION OF GAS LASERS TO STUDIES OF FUNDAMENTAL MOLECULAR AND ATOMIC PROCESSES.		5. TYPE OF REPORT & PERIOD COVERED Final 1 July 1975-15 Nov. 1979 6. PERFORMING ORG. REPORT NUMBER 83259
7. AUTHOR(s) Professor Ali Javan		8. CONTRACT OR GRANT NUMBER(s) N00014-76-C-0447
9. PERFORMING ORGANIZATION NAME AND ADDRESS Department of Physics Massachusetts Institute of Technology Cambridge, Massachusetts 02139		10. PROGRAM ELEMENT, PROJECT, TASK AREA & WORK UNIT NUMBERS Task NR 395-504
11. CONTROLLING OFFICE NAME AND ADDRESS Dr. William J. Condell, Jr., Office of Naval Research, Dept. of Navy Arlington, Virginia 22217		12. REPORT DATE 12 May 1980 13. NUMBER OF PAGES 82
14. MONITORING AGENCY NAME & ADDRESS(if different from Controlling Office) (Same)		15. SECURITY CLASS. (of this report) Unclassified 15a. DECLASSIFICATION/DOWNGRADING SCHEDULE

16. DISTRIBUTION STATEMENT (of this Report)

Unlimited

17. DISTRIBUTION STATEMENT (of the abstract entered in Block 20, if different from Report)

(Same)

18. SUPPLEMENTARY NOTES

19. KEY WORDS (Continue on reverse side if necessary and identify by block number)

Excimer
Photopreionization
Multifrequency laser
Highly stripped atoms
High pressure gas laser

20. ABSTRACT (Continue on reverse side if necessary and identify by block number)

Several topics are summarized in the areas of excimer ground state kinetics, coherent pulse evolution in a CO_2 amplifier, photopreionization and operation of a multi-atmosphere TEA laser, relaxation of He_2 excimers and highly stripped atoms.

continued.....

DD FORM 1 JAN 73 1473 EDITION OF 1 NOV 65 IS OBSOLETE
S/N 0102-LF-014-6601

Unclassified

SECURITY CLASSIFICATION OF THIS PAGE (When Data Ent

Very significant pioneering progress was made in the area of XeF ground state kinetics, demonstrating the nature and measuring parameters of ground state dissociation.

Coherent reshaping of short duration CO_2 laser pulses in a low pressure longitudinal discharge amplifier is studied for a variable number of gain lengths (up to 7). Pulses grow in duration and amplitude as theoretically predicted. The transverse relaxation parameter, T_2, and zero degree pulses are studied from pulse evolution data.

Photopreionization by flashlamp and seed gas are studied in N_2 lasers at presures up to atmospheric.

A sealed multiatmospheric CO_2 TEA laser is reported in which recombination of principle discharge products CO and O_2 is induced by recirculating the laser gas mixture through a room-temperature oxide catalyst bed. No special gas mixtures are required and catalyst is compatible with at least some trialkylamine seed gases.

The fine structure splitting of the $e^3\Pi g$ state was studied for the first time. Optical-optical double resonance with co-propagating beams from a nitrogen laser pumped dye laser with two output wavelengths was used to obtain doppler-free fluorescence signals.

Experimental study of charge transfer between highly stripped ions of carbon and noble-gas atoms was conducted. One-and two-electron transfer to C^{+3}, C^{+4} and C^{+5} was observed. The ions were obtained from plasma generated by a pulsed high-power CO_2 laser.

TABLE OF CONTENTS

	Page
Summary of Research	1
XeF Ground State Kinetics-Final Report	4
Multifrequency CO_2 Laser	8
High Pressure Gas Lasers Emphasing Tunability	9
Appendix A - Coherent Optical Pulse Evolution in a CO_2 Amplifier and Relaxation Studies of He_2 Excimers using Dye Laser Techniques	
Appendix B - Highly Stripped Atoms	
Appendix C - Excimer	
Appendix D - Photopreionization	
Appendix E - Thesis Abstracts of Students Supported by ONR Contract Funds	

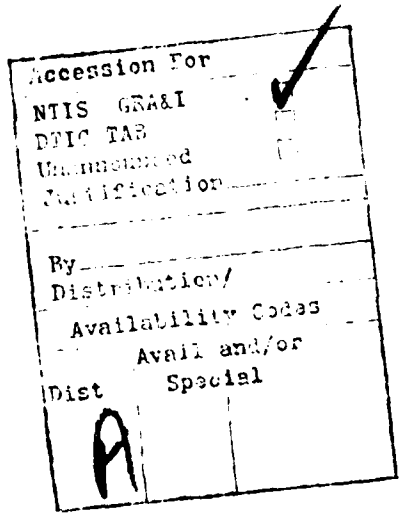

1. Summary of Research

This report covers the duration of ONR Contract with MIT, number N00014-76-C-0447, Task: NR 395-504 which extended from 1 July 1975 through 15 November 1979.

Several topics are summarized in the areas of excimer ground state kinetics, coherent pulse evolution in a CO_2 amplifier, photopreionization and operation of a multi-atmosphere TEA laser, relaxation of He_2 excimers and highly stripped atoms.

XeF ground state kinetics is the subject of section 2 as well as the three published articles in Appendix C and the thesis abstract of Stephen Fulghum (Appendix E-2). Very significant pioneering progress was made in this area demonstrating the nature and measuring the parameters of dissociation of the ground state.

The coherent reshaping of short duration (2-5 nsec) CO_2 laser pulses in a low-pressure ($\sim$5 torr), longitudinal discharge CO_2 amplifier is studied experimentally in the linear regime for a variable number of gain lengths ($\alpha L \leq 7$). Single pulses grow considerably in duration as well as amplitude in agreement with theoretical considerations. Analysis of the observed pulse evolution is used to obtain the transverse relaxation parameter T_2. Zero-degree pulses $\left[\int_{-\infty}^{+\infty} E(z,t)\,dt = 0\right]$ are observed to terminate much of the long tail which occurs in single-pulse amplification. Off-resonant amplification of short-duration pulses is shown to lead to dramatic changes in the zero-degree pulse evolution. Numerical calculations relating to pulse amplification in the nonlinear regime for high-pressure CO_2 amplifiers are also presented.

This material is covered in more detail in Appendices A and E-6.

Photopreionization of the 3371-Å pulsed N_2 laser by use of a seed gas of low ionization threshold and flashlamp excitation is observed to result in increased laser output and reproducibility. Preionization also increases the range of permissible operating pressures, enabling operation with atmospheric-pressure mixtures of N_2 and He without reduced intensity.

A sealed multiatmospheric CO_2 TEA laser is reported in which recombination of principle discharge products CO and O_2 is induced by recirculating the laser gas mixture through a room-temperature oxide catalyst bed. No special gas mixtures are required and the catalyst is compatible with at least some trialkylamine seed gases.

Additional material in included as Sections 3 and 4 and Appendices D and E-3.

Doppler-Free Spectroscopy of the Helium Excimer Molecule

The $e^3\pi_g$ state of the molecular He_2 excimer was studied. Previous work clarified and established the kinetics and radiative lifetime of this state. It is thus possible to resolve the fine structure of the $e^3\pi_g$ state. These fine structure splittings have not been seen in conventional spectroscopy because they are less than the doppler width of He_2 which is about 3 GHz. By means of optical-optical double resonance with copropagating beams, doppler-free fluorescence signals can be obtained. A nitrogen laser pumped pulsed dye laser was made to have an output in two narrow frequency regions. When a fine structure splitting

of the He_2 molecular $e^3\pi_g$ state has an energy equal to the difference in energy of the two frequencies from the dye laser, an enhanced fluorescence signal was observed. It was then possible to change the magnitude of the difference frequency of the dye laser by scanning the passive or active Fabry-Perrot etalon and obtain the fine structure spectrum of the molecule. Alternatively, we could hold the difference frequency of the dye laser at a suitable value, and tune the fine structure of the He_2 by applying a changing magnetic field to the helium cell.

Additional discussion may be found in Appendices A and E-1.

Experimental study of charge transfer between highly stripped ions of carbon and noble-gas atoms was conducted. One-and two-electron transfer to C^{+3}, C^{+4} and C^{+5} was observed. The ions were obtained from plasma generated by a pulsed high-power CO_2 laser. This work is covered in considerable detail in Appendices A and E-4.

2. XeF Ground State Kinetics

Final Report

This report is an overview of the research done at MIT on the kinetic processes in the XeF ground electronic state. Specific results and conclusions can be found in the three papers in the appendix.

The primary goal of this effort has been the direct measurement of vibrational equilibration rates and direct dissociation rates in the XeF ground state vibrational manifold. Knowledge of these rates is essential to a full understanding of XeF laser processes, particularly in predicting maximum efficiencies and other laser behavior at pulse lengths greater than about 100 nanoseconds. It is at these longer pulse lengths that population can build up in the vibrational levels of the ground state and cause effects such as the shift of laser output from one transition wavelength to another.

Previous estimates of the XeF ground state kinetic rates relied primarily on indirect information. The entire ground state vibrational manifold was treated as a single level and a

"lifetime" for this level was chosen to explain observed efficiencies. Such techniques are susceptible to considerable error since many factors (some undoubtedly unrecognized) are involved in absolute efficiency measurements. Our experiments were the first to measure kinetic rates directly, both in XeF produced by a laser discharge and in XeF produced by photodissociation (which eliminates many uncertainties connected with the discharge).

Another very important part of this work has been the development of a multilevel model of the ground state vibrational manifold. It provides a means of describing important laser behavior such as the competition between transitions terminating on different vibrational levels of the ground state. The development of this model involved choosing theoretical descriptions of the kinetic processes that used parameters which could be determined directly from the experimental data. Thus the multilevel model is well based in both theory and experiment. It also provides a means by which the results of many different experiments can be compared such as showing how the "lifetime" of a single level model actually relates to the kinetic processes in the real vibrational manifold.

A fruitful line of continuation on this project would be the direct determination of the effects of temperature on these processes. We have used the theoretical models to extrapolate our room temperature measurements to 450°K in

order to model the observed increases in laser efficiency at these temperatures (see paper 3). The importance of understanding this increased efficiency justifies repeating our type of measurement at higher temperatures. Another possibility (which would take advantage of equipment already constructed) is a search for lasing in the 50 micrometer region which probably occurs due to transient population inversions in the vibrational levels of the ground state. Such processes could act as relaxation mechanisms in actual XeF lasers. The information could also provide more exact measurements of spectroscopic parameters in the ground state.

Publications

Two papers have been published describing this work. The final paper is scheduled for publication in August 1980 in the Journal of Quantum Electronicss. All three are enclosed. In addition, four presentations have been made at conferences during the course of these experiments.

S.F Fulghum, I.P. Herman, M.S. Feld and A. Javan "XeF Ground State Dynamics" paper DA-2, 31st Annual Gaseous Electronics Conference, Buffalo, NY, 17 Oct 78

S.F. Fulghum, I.P. Herman, M.S. Feld and A. Javan
"XeF Ground State Dynamics in a Laser Discharge"
paper TuA7, OSA Annual Meeting, San Francisco, CA,
31 Oct 78

S.F. Fulghum, M.S. Feld and A. Javan
"A Multilevel model of XeF Ground State Kinetics"
and
"A Model of XeF Laser Oscillation with a
Multilevel Ground State"
both papers presented at the 32nd Annual Gaseous
Electronics Conference, Pittsburgh, PA, 9-12 Oct 79

3. Multifrequency CO_2 Laser

Using a multiline laser, work has continued on the experiment to excite high vibrational levels in a molecule. The molecule first chosen for investigation is D_2O, whose vibration (bending mode) has frequencies resonant with the 9 μm band of the CO_2 laser. To study the energy redistribution, a step-by-step study was made to determine which vibrational energy differences are resonant with the CO_2 frequencies. Since the D_2O was studied at a pressure greater than 10 Torr, the rotational levels were assumed to be completely thermalized; therefore, it was not necessary to be on resonance with only common rotational levels. A low-power cw CO_2 laser was used as a probe to find the resonant transitions of each succeeding vibrational level. Once the required frequencies are known, the multifrequency laser will be set to these frequencies and used to force high vibrational heating of the D_2O molecule. This will confirm CO_2 laser-D_2O transition coincidences and also the various corresponding molecular relaxation rates. For the correct multifrequency pulse width and energy, substantial amounts of D_2O should be dissociated into OD and D. The amount of OD produced will be measured by the use of CO as a scavenger, producing CO_2. The CO_2 will be measured by standard spectroscopic techniques.

4. High Pressure Gas Lasers Emphasing Tunability

Several significant steps in development of continuously-tunable pulsed CO_2 lasers have been taken. This device requires a pressure of 10-15 atm in the CO_2 laser discharge to pressure-broaden the lines sufficiently that they overlap. The desired operating wave length is then selected by a tunable optical cavity containing a diffraction grating as the frequency-selective element.

A laser designed for pressures up to 15 atm was operated reliably up to seven atmospheres at repetition rates of 5-10 Hz early in the program. At this time the limit on operating pressure was due to the available voltage of the pulse generator. A new 75 KV spark-gap type pulse generator was built, permitting operation at the design pressure. The laser amplifying medium is established between two 25 cm. long Rogowski-profile electrodes separated by 0.6 cm with a discharge width of about 1 cm, giving an active volume of 15 cm^3. The system was designed so that it could be easily modified to incorporate transverse gas circulation and cooling for higher repetition rates. Preionization energy was provided by two segmented transmission lines parallel to the sustainer electrodes and displaced 3.5 cm from the center of the discharge region. Each segmented line produces 26 arcs spaced about 1 cm apart along its length. The containment vessel is clear lucite reinforced with aluminum top and bottom plates. Beam entry and exit is via internal 6 mm-thick Brewster-angle NaCl windows. Each preionization "sparkrod" is driven by a

3600 pF $BaTiO_3$ capacitor charged to 10 KVDC (180 mJ) at the end of a 1 meter length of RG-58/U 50Ω coaxial transmission line. The two capacitors are switched simultaneously by a single hydrogen thyratron.

A grating with 150 grooves/mm gave a continuous frequency scan from P(22) of the 10.6 μ band to P(24) of the same band with no noticeable frequency pulling at a pressure as low as 10 atmospheres in the laser.

A heated absorption cell was assembled and a frequency scan of the P(24) line of the 10.6μ band was made for various pressures of pure CO_2, yielding an estimate of about 4 GHz for the laser full width. A larger grating with beam expanding telescope was also used with the high pressure discharge and experiments were undertaken to measure the narrowing of the laser linewidth caused by the ten-fold expansion of the usable grating area associated with the telescope.

The high voltage pulsing system was then modified to reduce the electrical noise pickup on the laser pulse detection electronics. Design and construction was also started on a transverse-flow cooling coil recirculating system, which allows increased pulse repetition rates. Recent efforts on the high-pressure CO_2 laser have been directed towards making it a more reliable and convenient spectroscopic research tool. The often-troublesome high-voltage pulse generator was ultimately replaced by an entirely new pulse of unique design and an electronically adjustable grating mount was added for precisely controllable

frequency scanning. Several other minor improvements have also been made. The one significant problem that remains unsolved is the eventual power damage to one of the ZnSe lenses in the beam-expanding telescope.

The laser can be operated anywhere in the 1-17 atmosphere range. It has an output linewidth on the order of $0.05cm^{-1}$ (1500 MHz), an output energy of up to 100 mJ, and a pulse repetition rate of 1-2 Hz.

This laser is primarily a spectroscopic tool although some short-pulse generation experiments have been done. Currently experiments are being conducted involving absorption in methyl halides (CH_3Cl, CH_3,Br, etc.) in the 10 μ region. In addition attempts are being made to resolve absorption lines of the two isotopic species of methyl chloride, CH_3Cl^{35} and CH_3Cl^{37}.

APPENDIX A

Coherent Optical Pulse Evolution in a CO_2 Amplifier (Optics Communications, 17, 32 (1976) and Relaxation Studies of He_2 Excimers using Dye Laser Techniques

COHERENT OPTICAL PULSE EVOLUTION IN A CO_2 AMPLIFIER

S.M. HAMADANI, N.A. KURNIT* and A. JAVAN
Massachusetts Institute of Technology, Cambridge, Massachusetts 02139, USA

Received 4 December 1975

The coherent reshaping of short duration (2–5 nsec) CO_2 laser pulses in a low-pressure (~ 5 torr), longitudinal discharge CO_2 amplifier is experimentally studied in the linear regime for a variable number of gain lengths ($\alpha L \lesssim 7$). Single pulses grow considerably in duration as well as amplitude in agreement with theoretical considerations. Analysis of the observed pulse evolution is used to obtain the transverse relaxation parameter T_2. Zero-degree pulses [$\int_{-\infty}^{\infty} E(z, t)\,dt = 0$] are observed to terminate much of the long tail which occurs in single-pulse amplification. Off-resonant amplification of short-duration pulses is shown to lead to dramatic changes in the zero-degree pulse evolution. Numerical calculations relating to pulse amplification in the nonlinear regime for high-pressure CO_2 amplifiers are also presented.

1. Introduction

In previous work [1–3] we have examined the evolution of short-duration optical pulses in an absorbing medium. In particular, a 180° phase reversal introduced in an optical pulse so as to form a zero-degree [4] pulse was observed to result in amplification of the phase-reversed portion of the pulse for times comparable to the transverse relaxation time. In this letter we extend these observations to the case of an amplifying medium and demonstrate that the long tail which results from amplification of a short-duration pulse can be terminated by application of a suitable phase-reversed pulse. While these observations are made in the linear intensity regime, similar considerations are shown to apply in the nonlinear regime as well. The use of 2–5 nsec input pulses to a low-pressure CO_2 amplifier allows observation of effects which would be important in the amplification of subnanosecond pulses in high-pressure amplifiers**. Off-resonant amplification of short-duration pulses is also studied by tuning the laser to oscillate in the wing of the gain profile, leading to dramatic changes in zero-degree pulse evolution due to the resultant frequency chirp [6].

2. Linear analysis

The shape and duration of the output pulse from a high-gain laser amplifier is dependent on a number of factors such as the gain medium's saturation behavior, bandwidth and dispersion, in addition to the input pulse shape and intensity. In the low-intensity linear regime, Fourier techniques can be applied to describe the pulse evolution [7]. In this regime the field produced at a depth z in an amplifier with gain coefficient α by a δ-function input of small area [8] $\theta_0 \ll 1$ is given by [7,9]

$$\frac{\mu E(z,t)}{\hbar} = \theta_0 \delta(q) + \theta_0 \frac{U(q)}{T_2}\left(\frac{\alpha z}{2q}\right)^{1/2} e^{-q} I_1\left[(2\alpha z q)^{1/2}\right], \tag{1}$$

where I_1 is a modified Bessel function, $q = (t - \eta z/c)/T_2$ is the retarded time normalized to the transverse re-

* Present address: Los Alamos Scientific Laboratory, University of California, Los Alamos, New Mexico 87544, USA.

** The tailoring of input pulses to generate short duration high power laser pulses of desired shape has been discussed by Goldstein and Hopf [5].

laxation time T_2 [‡], and $U(q)$ is the unit step function.

Eq. (1) is derived for a rectangular input pulse of of amplitude E_0 and duration τ, in the limit $\tau \to 0$ with

$$\theta_0 \equiv \int_{-\infty}^{\infty} dt\, \mu E(0,t)/\hbar = \mu E_0 \tau/\hbar$$

held constant. The response to experimental input pulses of width $\tau \ll T_2$ is well approximated by eq. (1) until the condition $\theta(z) \ll 1$ is violated. Note that eq. (1) describes a pulse given by the incident δ-function followed by a "tail" which starts at an amplitude $\mu E/\hbar = \alpha z \theta_0/2T_2$. For $\alpha z \ll 1$, the tail decays as e^{-q}, i.e., at fixed z as e^{-t/T_2}, which characterizes the decay of the induced polarization for this thin slab limit. For larger αz, the exponential tail is further amplified by successive regions of the gain medium, until for $\alpha z \gg 1$, eq. (1) takes the characteristic form indicated in the upper trace of fig. 1a. For large αz, the pulse grows to a peak value

$$\mu E_p/\hbar \simeq (\theta_0/T_2)(2\pi\alpha z)^{-1/2} \exp(\tfrac{1}{2}\alpha z), \qquad (2)$$

at a time

$$\tau_p \simeq \tfrac{1}{2}(\alpha z - 3)T_2. \qquad (3)$$

and decays to 1/e of this peak in a time $\sim(2\alpha z)^{1/2}\, T_2$. These results hold when the argument of I_1 is sufficiently large that $I_1(x)$ can be approximated by $e^x/(2\pi x)^{1/2}$.

In this linear intensity regime, the amplification of a short duration pulse through a large number of gain lengths is thus seen to lead to an output pulse whose duration (and hence phase memory of the input) is greater than $\frac{1}{2}\alpha z T_2$. The relative phase of successive input pulses is thus important in determining the output pulse shape for pulses separated by as much as $\frac{1}{2}\alpha z T_2$ rather than just T_2 [‡]. In the case of strongly saturating pulses, the pulse narrows due to the gain reduction in the tail [11], but rapid population equilibrium can still lead to a long tail [12].

Input pulses of longer duration undergo a similar evolution, but there is now a growth of the pulse amplitude during the input pulse. In the linear regime, analytic solutions for rectangular pulses of arbitrary duration as well as certain other shapes can be written as a sum of Bessel functions [7], or numerical solutions can be generated for arbitrary input pulse shapes from the impulse response of eq. (1).

3. Single-pulse amplification

Experimental traces showing the amplification of small area ($\sim \pi/500$), 2-nsec CO_2 input pulses in a low-pressure CO_2 amplifier are given in fig. 1b for two values of αL. The amplifying medium of length $L = 3.4$ m consists of two 2.5-cm diameter, 1.7-m long, longitudinal discharge tubes operated at a pressure of ~ 5 torr (1:1:2 CO_2–N_2–He). The oscillator and amplifier tubes are repetitively pulsed [☆] for higher gain. The laser produces ~ 10 W, 200 μsec pulses at a 100 Hz rate. A portion of this radiation is switched into the perpendicular polarization by a GaAs electrooptic switch and Ge analyzer [1] and sent to the amplifier. The output pulses are detected with a high speed Cu:Ge detector through a 10% attenuator to prevent oscillation of the high gain amplifier due to feedback from the detector.

In the linear regime both αL and T_2 can be uniquely determined from an accurate knowledge of the

[‡] The simple form given in eq. (1) results from approximating the inhomogeneous contribution to the lineshape as a lorentzian so that $1/T_2 = 1/T_2^* + 1/T_2'$ where T_2' is the homogeneous relaxation time. We have written $\alpha = 2\alpha_0 T_2 = 4\pi N\mu^2 \omega T_2/\hbar nc$ in the notation of ref. [7]. For a gaussian inhomogeneous line of 1/e half-width $\Delta\omega_D$, this expression for the peak gain coefficient α remains valid in the limits $T_2' \ll T_2^*$ or $T_2^* \ll T_2'$ provided one defines $T_2^* \equiv \sqrt{\pi}/\Delta\omega_D$. For intermediate values, the effective T_2 which gives the correct α must be obtained from $T_2 = (T_2^* a/\pi) \times \int_{-\infty}^{\infty} dx \exp(-x^2)/(a^2 + x^2)$, where $a = 1/\Delta\omega_D T_2'$.

[‡] The effect of high gain on decreasing the influence of inhomogeneous (T_2^*) dephasing on pulse evolution has been discussed in connection with the superradiant decay of an inverted system by Herman et al. [10]. In their case, the collisions responsible for T_2' also resulted in depopulations of the inverted level since only one rotational level was initially excited. Thus pulses could not evolve over times long compared to T_2'. In the present case, the rotational relaxation processes have the effect of restoring the initial inversion, so the high gain makes it possible for pulses to evolve over times long compared to T_2' as well as T_2^*.

[☆] Pulsing the discharge with a low duty factor prevents excessive heating of the gas. A small chirp of ~ 10 kHz/μsec, which is negligible on the time scale of these experiments, also results from pulsing the discharge.

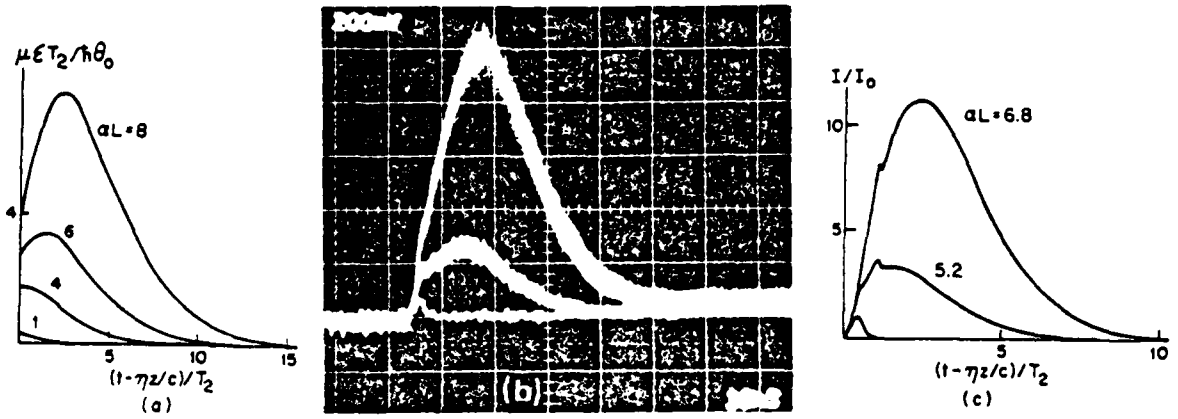

Fig. 1. Theoretical plots and experimental pulse-shapes for short pulse amplification in the linear regime.
(a) Electric field [eq. (1)] produced by an amplifier in response to a δ-function input pulse of area θ_0 as a function of normalized retarded time for $\alpha L = 1, 4, 6$ and 8.
(b) Multiple exposure photograph showing amplification of small area ($\pi/500$) 2-nsec CO_2 input pulse (lower trace) in low pressure CO_2 amplifier for two values of αL obtained by changing the discharge voltage (10-nsec/div).
(c) Intensity profiles generated from the impulse response of (a) for a pulse of duration (fwhm) $\tau = 0.4 T_2$ and peak intensity I_0.

input and output pulse amplitudes and shapes (which may require deconvolution of the detector response). The gain can be determined from the areas under the square root of the observed intensity curves (fig. 1b) by means of the area theorem [8], which in the linear regime can be written:

$$\theta(z) = \theta_0 \exp(\tfrac{1}{2}\alpha z). \qquad (4)$$

This expression has been shown [7] to hold in the presence of both homogeneous and inhomogeneous broadening when population changes are negligible. The ratio of the areas obtained from the square root of the intensities in fig. 1b are $\alpha L = 6.8 \pm 0.2$ for the upper trace, corresponding to a maximum gain coefficient of 0.02 cm^{-1}, and $\alpha L = 5.2 \pm 0.2$ for the lower trace*. Fig. 1c shows the amplifier output for these values of αz as calculated from the impulse response of eq. (1) for our experimental pulse shape. The delay, τ_p, of the peak of the output beyond the peak of the input pulse allows determination of T_2 through eq. (3), or, more accurately, by matching the experimental curves in fig. 1b to curves like those in fig. 1c. Note that τ_p is insensitive to the input pulse shape and duration τ if $\tau \ll \tau_p$. We obtain $T_2 = 5.0 \pm 0.5$ nsec. This value is in agreement with that calculated (see footnote ‡ on p. 33) for $T_2' = 9.4$ nsec for our gas mixture‡ if we assume $T_2^* = \sqrt{\pi}/\Delta\omega_D = 8.0$ nsec, corresponding to a temperature of 370 K. A further check on the self-consistency of these results as well as the assumption that the system remains linear is obtained from the ratio of the peak output/input intensities, which depends on both αL and τ/T_2 [cf. eq. (2) with $\theta_0 = \mu E_0 \tau/\hbar$]. The calculated intensities in fig. 1c with $\tau = 0.4\, T_2$ are in good agreement with the observed intensities of fig. 1b after correction for the effect of the amplified background*.

* There is a small amplified background field present resulting from leakage through the electrooptic switch (the baseline is suppressed in fig. 1b, but shown in fig. 2a). This modifies the peak amplitude observed for the short pulse in these experiments. The values of αL obtained from fig. 1b have been corrected to take into account this difference.

4. Zero-degree pulse amplification

Fig. 2a shows the modification of the amplified 2 nsec pulse of fig. 1b by an equal but out-of-phase

‡ The collision-broadening coefficients used are those given by Abrams [13] with a small correction for gas temperature.

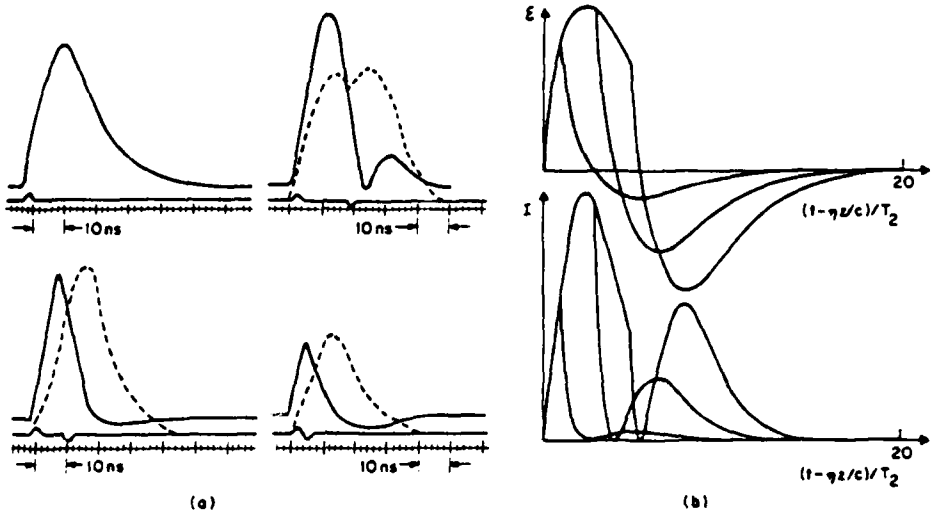

Fig. 2. Effect of pulse separation and initial frequency offset on amplification of 2 nsec zero-degree pulses.
(a) Oscilloscope traces showing modification of the amplified 2 nsec pulse of fig. 1b as an equal but out of phase pulse is added with variable delay (solid curves). Baseline shift shows the amplification of background due to leakage through electrooptic switch. Dashed curves show the evolution of initially off-resonant pulses.
(b) Electric fields E and intensities I calculated by subtracting the electric field produced by the second pulse from that due to the first for two out-of-phase input pulses of length $\tau = 0.4\,T_2$, with $\alpha L = 6.8$ and delays of 1, 3 and 5 T_2.

pulse is added with variable delay. A 180° phase shift is electrooptically introduced between the two pulses in the manner described in ref. [1]. Since the two input pulses give approximately zero area, the area of the output [eq. (4)] remains near zero. The second, smaller and broader output pulse in fig. 2a is out-of-phase with the first so as to maintain zero area. For the lower curves in fig. 2a, this secondary lobe is evident as an undershoot due to interference with the amplified background. In this linear regime, the resultant output pulse can be calculated as shown in fig. 2b by subtracting the electric field produced by the second pulse from that due to the first. If the input pulses are close together, destructive interference leads to a short first lobe and (for a zero-area input pulse) a small, broad second lobe of equal area but much smaller energy, in agreement with the lower curves of fig. 2a. For two in-phase 2 nsec input pulses of equal area (not shown), the output pulse is increased in amplitude but not appreciably in width, in agreement with eqs. (3) and (4). Similar results have also been observed with 5 nsec square pulses for which $\tau \simeq T_2$.

5. Off-resonant pulse amplification

Also shown in fig. 2a (dashed curve) is the evolution of initially off-resonant pulses obtained by tuning the laser to oscillate in the wing of the gain profile. In this case, the output chirps onto resonance after the input is terminated [6]. The 180° phase shift between the two pulses is not preserved and there is no longer cancellation between the resultant fields. It should be noted that the output pulse has nearly the same amplitude for the off-resonance case, but the amplified background* (baseline shift in fig. 2a), is significantly reduced. The use of off-resonant input pulses can thus be of importance for limiting the amplification of background radiation as well as for generating chirped pulses which may be useful for pulse compression.

* See footnote * on previous page.

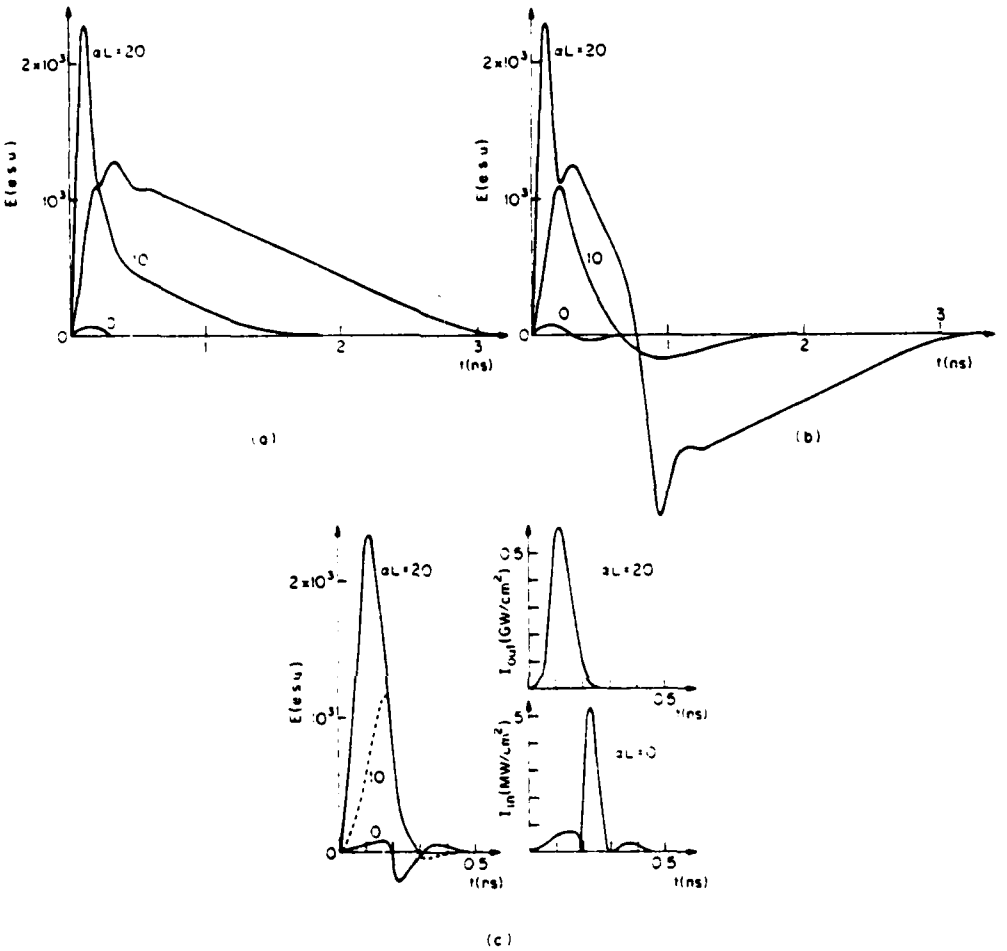

Fig. 3. Numerical calculations for pulse evolution in the nonlinear regime for high pressure CO_2 amplifier. $T_1 = 2T_2 = 0.2$ nsec.
(a) Amplification of $\pi/10$, 0.2 nsec input pulse.
(b) For $\alpha L = 10$, the long tail in (a) is reduced by a second out-of-phase pulse of smaller area ($\pi/25$), but for higher gain the second pulse itself develops into the characteristic shape of (a).
(c) The tail is completely suppressed by using as input three pulses of alternate phase and tailored shape.

6. Nonlinear regime

For efficient energy extraction from an amplifying medium, it is desirable to drive the medium into saturation, where this linear analysis is not applicable. However, if one also wants an appreciable increase in energy per stage of amplification, the input pulse will not generally be strongly saturating and the initial growth will be as described above. Furthermore, rapid population equilibration, due in CO_2 to rotational cross relaxation, prevents complete saturation and attendant pulse sharpening [14] unless multiline operation is used [15]. Typical calculations [12] show that high-power CO_2 pulses can be expected to develop a characteristic intense spike followed by a long tail which carries a significant fraction of the total energy. This behavior is illustrated in fig. 3a which shows the amplification of a ($\pi/10$) 0.2 nsec input

pulse into the nonlinear regime, calculated from the coupled Bloch--Maxwell equations [8] with $T_1 = 2T_2 = 0.2$ nsec. In these calculations we have made the simplifying assumption that the medium consists of homogeneously broadened two-level molecules whose population relaxes to equilibrium (determined by the ratio of pump to decay rates) with a single relaxation time T_1 [#].

If the input pulse is followed by a similar out-of-phase pulse of the same area, the tail of the first pulse is suppressed as discussed above. However, for sufficiently high gain, the second pulse itself develops into the characteristic shape of fig. 3a. By reducing the amplitude of the second pulse, it is possible to suppress the tail of the first pulse while limiting the growth of the second pulse, as shown in fig. 3b for a $(\frac{1}{10}\pi - \frac{1}{25}\pi)$ pulse. Such pulses can be realized by the method of ref. [1]. However, it should be noted that as the ratio of the areas is made smaller, the effect of the second pulse is delayed. In order to completely suppress the tail, it is necessary to use input pulses of carefully tailored shape which can be determined by the method of ref. [5] [##]. Fig. 3c shows the output obtained using a triply-lobed input of total area $\pi/100$ for which the first lobe of area $\sim \pi/14$ grows to saturation for $\alpha L \gtrsim 15$. The second out-of-phase lobe of larger area ($\sim \pi/11$) but smaller width suppresses the tail of the first pulse but would itself develop into a strongly saturating pulse were it not followed by the third lobe (of area $\sim \pi/36$). Also shown in fig. 3c are the intensity profiles for the input (lower right) and $\alpha L = 20$ output (upper right) pulses. Multiple lobed pulses of the type shown in fig. 3c can be experimentally obtained by coherent pulse propagation in a resonant absorber [3].

[#] This assumption is equivalent to considering an infinite rotational reservoir model, which does not allow for saturation of the entire manifold of rotation levels. This will somewhat overestimate the growth of the tail, but nevertheless gives results similar to the more detailed model considered in ref. [12]. In this calculation we also ignore the effects of linear loss terms, which are discussed, for example, by Icsvegi and Lamb [16].

[##] In using this method one should be aware that small (and perhaps insignificant) changes in the desired output can require major changes in the input pulse-shape. This is particularly true if fast rise and fall times are desired.

Acknowledgements

We wish to thank M.S. Feld and J.C. MacGillivray for useful discussions.

References

[1] H.P. Grieneisen, J. Goldhar, N.A. Kurnit, A. Javan and H.R. Schlossberg, Appl. Phys. Lett. 21 (1972) 559.
[2] H.P. Grieneisen, J. Goldhar and N.A. Kurnit, in: Proc. Third Rochester Conf. Coherence and Quantum Optics, eds. L. Mandel and E. Wolf (New York, Plenum, 1973) p. 5.
[3] S.M. Hamadani, J. Goldhar, N.A. Kurnit and A. Javan, Appl. Phys. Lett. 25 (1974) 160.
[4] C.K. Rhodes, A. Szöke and A. Javan, Phys. Rev. Lett. 21 (1968) 1151;
F.A. Hopf, C.K. Rhodes, G.L. Lamb Jr. and M.O. Scully, Phys. Rev. A3 (1971) 758;
G.L. Lamb Jr., Physica 66 (1973) 298.
[5] J.C. Goldstein and F.A. Hopf, Opt. Commun. 11 (1974) 118.
[6] M.D. Crisp, Appl. Optics 11 (1972) 1124;
J.C. Diels and E.L. Hahn, Phys. Rev. A8 (1973) 1084.
[7] M.D. Crisp, Phys. Rev. A1 (1970) 1604.
[8] S.L. McCall and E.L. Hahn, Phys. Rev. 183 (1969) 45.
[9] D.L. Bobroff and H.A. Haus, J. Appl. Phys. 38 (1967) 390.
[10] I.P. Herman, J.C. MacGillavray, N. Skribanowitz and M.S. Feld, Proc. Vail Conf. Laser Spectroscopy, June 1973, eds. R.G. Brewer and A. Mooradian (New York, Plenum, 1974) p. 408.
[11] L.M. Frantz and J.S. Nodvik, J. Appl. Phys. 34 (1963) 2346;
N.G. Basov, V.S. Zuev, P.G. Kryukov, V.S. Letokhov, Yu.V. Senatskii and S.V. Chekalin, Sov. Phys. JETP 27 (1968) 410;
P.W. Hoff, H.A. Haus and T.J. Bridges, Phys. Rev. Lett. 25 (1970) 82;
B.B. MacFarland, IEEE J. Quantum Electron. QE-9 (1973) 731;
N. Skribanowitz and B. Kopainsky, Appl. Phys. Lett. 27 (1975) 490.
[12] F.A. Hopf and C.K. Rhodes, Phys. Rev. A8 (1973) 912;
E. Fill and W. Schmid, Phys. Lett. 45A (1973) 145.
[13] R.L. Abrams, Appl. Phys. Lett. 25 (1974) 609.
[14] G.T. Schappert, Appl. Phys. Lett. 23 (1973) 319;
E.E. Stark Jr., W.H. Reichelt, G.T. Schappert and T.F. Stratton, Appl. Phys. Lett. 23 (1973) 322;
J.F. Figueira, W.H. Reichelt, G.T. Schappert, T.F. Stratton and C.A. Fenstermacher, Appl. Phys. Lett. 22 (1973) 216.
[15] B.J. Feldman, Opt. Commun. 14 (1975) 13;
J.F. Figueira, J.S. Ladish, J.T. Schappert and S.J. Thomas, Appl. Phys. Lett. 27 (1975) 591.
[16] A. Icsvegi and W.E. Lamb Jr., Phys. Rev. 185 (1969) 517.

RELAXATION STUDIES OF He_2 EXCIMERS USING DYE LASER TECHNIQUES

Department of Physics
Massachusetts Institute of Technology
Cambridge, Massachusetts 02139

The technique of laser-induced fluorescence using a pulsed dye laser has been applied to study processes in ground and excited triplet states of molecular helium. The technique is simple and generally applicable. In the present work it was used to study the formation and quenching of the ground triplet state He_2 ($a^3\Sigma^+_u$) = He_2^m and the relaxation processes of the He_2 ($e^3\Pi_g$).

In the experiment, a pulsed helium gas discharge is used to produce different excited species, some of which become He_2, which is then quenched by different mechanisms. A nitrogen laser pumped dye laser was used to excite the $a^3\Sigma^+_u$ (v,N)→ $e^3\Pi_g$(v,N') =4650Å vibronic transitions of He_2 in the afterglow of the gas discharge. The excitation was measured by monitoring the fluorescence emitted from the $e^3\Pi_g$ level of He_2. The detection system consisted of a filter followed by a cooled photomultiplier. The signal to noise ratio was further increased by using a gated integrator with an adjustable gate aperture time.

It was found in this work that He_2^m is produced mainly during the first 400μsec of the afterglow from excited helium atoms. Also the formation rate of He_2^m coincides with the destruction rate of He^+ through transformation to He_2^+ and dielectronic recombination. This model also explains the variation of peak current during the glow with peak population of He_2^m. The rate of formation of He_2 from He^+ was found to be (2.2 ± 0.3) times the concentration of He^+.

Of course the formation of He_2^m from He^+ could involve many other intermediate steps. In the experimental conditions of this work, other mechanisms that produce He_2^m are found to make very small contributions to the formation of He_2.

The main loss mechanism of He_2^m is diffusion to the walls. Another loss mechanism is electron quenching. The v=1 state was found to be quenched faster than v=0. The first one has a rate of $(9.00 \pm 2.90) \times 10^{-9}$ $cm^3/sec.$ while the v=0 has a rate of $(2.2 \pm 0.70) \times 10^{-9}$ $cm^3/sec.$ The dependence of this quenching rate on the vibrational quantum number was seen here for the first time.

It was also found that the lifetime "τ" of the $e^3\Pi_g$ state is given by $1/\tau = [37.22 \pm 8.5 + (4.30 \pm 1.20)\ p]\ 10^6\ sec^{-1}$ where "p" is the pressure in torr. It was also found that a collision of an excited molecule with a helium atom could change the electronic state of the molecule. This collision transfer allowed us to measure the radiative lifetime of the $e^3\Pi_g$, $d^3\Sigma^+_u$, $f^3\Sigma^+_u$ and $f^3\Pi_u$ states as being 27 ± 6, 53 ± 5, 27 ± 6, and 40 ± 13 nsec, respectively. The collision transfer rate from the $e^3\Pi_g$ to the $d^3\Sigma^+_u$, $f^3\Pi_u$ and $f^3\Delta_u$ was measured as being $(6.70 \pm 1.39) \times 10^6$, $(1.00 \pm 0.23)\ 10^6$ and $(22.6 \pm 5.2) 10^3$ $sec^{-1}torr^{-1}$ respectively. The collision transfer rate from the $e^3\Pi_g$ to the $f^3\Sigma^+_u$ was found to be extremely fast and such that at pressures above 3 torr the two levels were in thermal equilibrium. This rate was determined as being over 30×10^6 $sec^{-1}torr^{-1}$.

Ratios of Franck-Condon factors between the $e^3\Pi_g$ and $a^3\Sigma^+_u$ states were measured as $q_{00}/q_{01} = 21 \pm 1$ and $q_{11}/q_{12} = 9.84 \pm 0.30$.

APPENDIX B

Highly Stripped Atoms

Observations of one-and two-electron transfer from noble-gas atom to highly stripped carbon ions. Applied Physics Letters 29, 96 (1976).

Observation of one- and two-electron transfer from noble-gas atom to highly stripped carbon ions

J. Goldhar,* R. Mariella, Jr.,† and A. Javan

Department of Physics, Massachusetts Institute of Technology, Cambridge, Massachusetts 02139
(Received 1 March 1976; in final form 26 April 1976)

Experimental study of charge transfer between highly stripped ions of carbon and noble-gas atoms was conducted. One- and two-electron transfer to C^{+3}, C^{+4}, and C^{+5} was observed. The ions were obtained from plasma generated by a pulsed high-power CO_2 laser.

PACS numbers: 34.60.+z, 82.30.Fi, 31.70.Fn, 52.50.Jm

The study of charge-changing collisions between low-velocity ($E_{trans} \leq 2$ keV) multiply ionized atoms and neutral atoms or molecules has been of value in understanding the physics of curve crossings,[1] CTR,[2] and recently interest has been shown in this area due to possible applications such as x-ray lasers.[3] Previous experimentors have observed single-electron capture by multiply charged ions under single collision conditions[4,5]; in the present work the technique has been extended[6] to observe cross sections for one- and two-electron capture by C^{+3}, C^{+4}, and C^{+5} ions. The observation of a large ($\sigma \geq 5$ Å^2) cross section for two-electron capture for C^{+4} implies a resonant process which is only possible when the product is in an excited electronic configuration.

The apparatus is shown schematically in Fig. 1. Typically, a 1-J laser pulse of 10 nsec duration from a CO_2 laser system operating at 10.6 μ is focused on a graphite target *in vacuo*, thus producing plasma which is the source of multiply charged ions. Several slits and apertures collimate the expanding plasma and thus produce an ion-beam pulse. The electrostatic analyzer at the end of the first flight tube transmits only one velocity group for each ionic charge Z according to $v \propto \sqrt{Z}$. Because all of the ions are formed essentially instantaneously on the time scale by which flight times are measured, the various charged species would exhibit normal time of flights proportional to $1/\sqrt{Z}$. Thus, for each laser pulse, the ion beam which enters the charge-exchange cell consists of a sequence of pulses each of which is composed of a single ion species.

If a positive voltage V_1 is applied to the retarding grid after the cell, the time of flight is lengthened over the normal time for a charge group's arrival at the detector. The effect of the retarding grid is diminished, however, if the ion has undergone a single- or double-electron capture in the cell region, and thus each original charge group's arrival at the detector can be split by charge exchange into the successive arrivals of two or three pulses. Ions which underwent double-electron capture would be the first subgroup to arrive, followed by those which underwent single-electron capture, and followed finally by unchanged ions at their fully retarded time. A plot of the extent of double-electron capture versus cell pressure of He in Fig. 2 clearly shows linear dependence, implying a single collision process. C^{+5} has no sizable two-electron capture cross section. The C^{+5} which underwent single-electron capture with Ar produced a C^{+4} and, since single-electron capture cross section for C^{+4} with Ar is large, a significant fraction (~25%) of these underwent a second collision—accounting for two peaks produced from C^{+5}.

The ion beam passing through the region after the

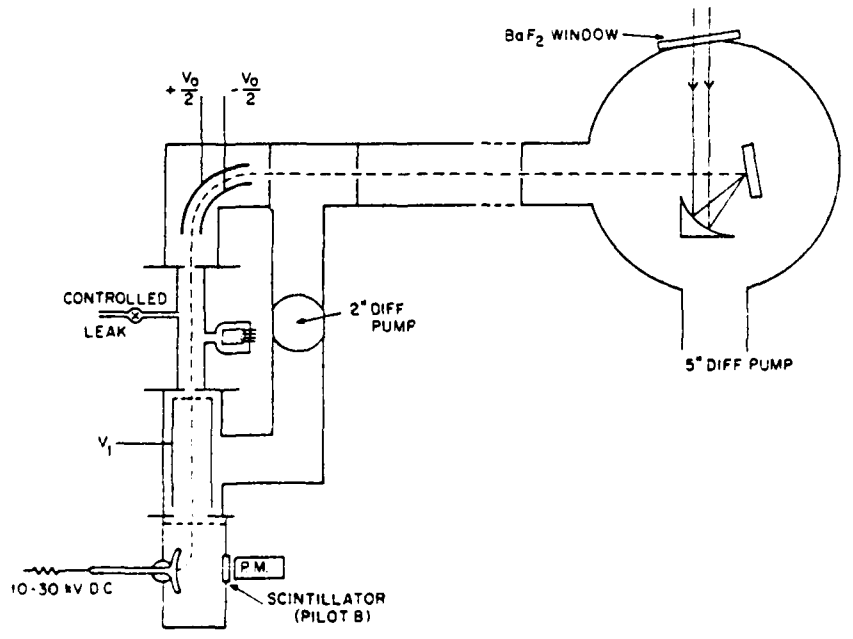

FIG. 1. Schematic of the apparatus used for charge-transfer measurements.

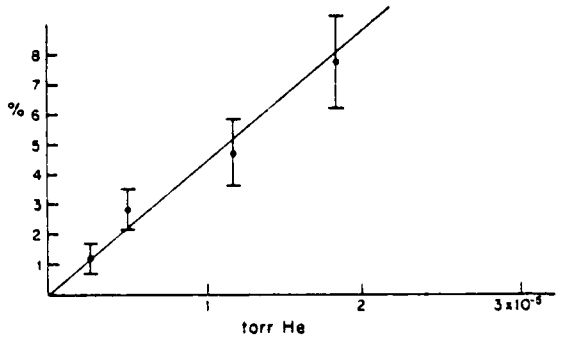

FIG. 2. Yield of C^{+2} from C^{+4} versus helium pressure in the cell.

gas cell is attenuated due to the finite divergence of the beam. This attenuation was determined at a number of voltage settings on the retarding grid. Combining the measured attenuation values with the small variation in detector efficiency for different charged species[6,7] it was possible to calculate absolute cross sections for the electron capture collisions. For C^{+4} collisions with Ar our single-electron capture cross section agrees with the previous measurement by Zwally and Koopman.[5] Our observation of somewhat larger one-electron pickup cross sections from He and Ne could be due to presence of metastable C^{+4} ions in the beam, since our ion source was a higher-temperature plasma.

TABLE I. One- and two-electron transfer cross sections in units of 10^{-16} cm^2 ± 20% uncertainty.

	He		Ne		Ar	
	1 electron	2 electron	1 electron	2 electron	1 electron	2 electron
C^{+3}	14	0[a]	12	0[a]	10	10
C^{+4}	1	5	4	23	56	16
C^{+5}	30	0[a]	70	0[a]	20	0[a]

[a] See text.

Table I shows the measured cross sections for single- and double-electron capture collisions with He, Ne, and Ar. Although single-electron capture is expected, in general, to predominate over double-electron capture, a careful examination of the relevant energy levels explains why this is not the case for C^{+4} collisions. For resonant charge exchange with ions in our velocity range, a final state (at infinite ion separation) must be typically 10—20 eV (the "energy defect") below the initial state (at infinite separation) so that Coulomb repulsion between final-state ions causes the initial- and final-state potential curves to cross at a reasonable (several Å) internuclear separation. For single-elec-

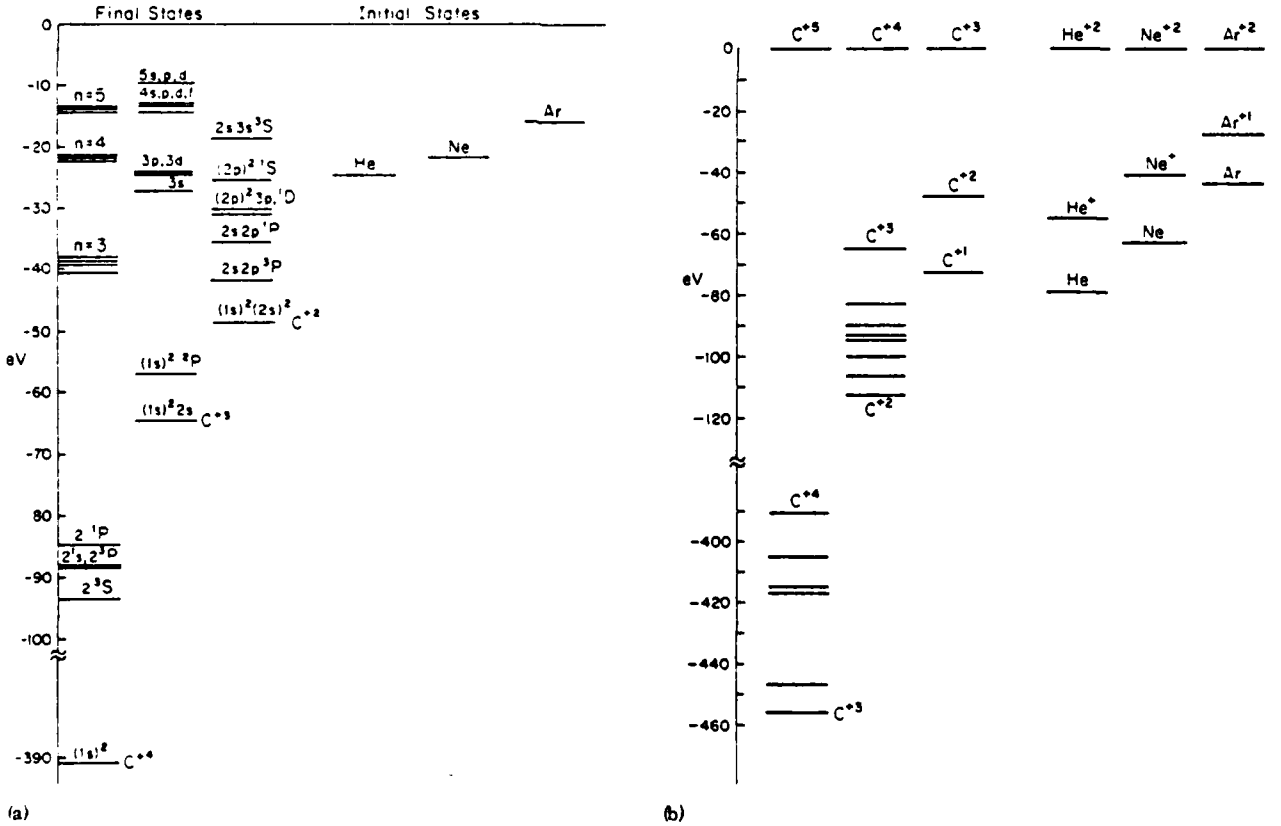

FIG. 3. Energy levels of the initial and final states for (a) single-electron and (b) double-electron transfer. [Taken from C.E. Moore, *Atomic Energy Levels*, Natl. Bur. Stand. Circ. No. 467 (U.S. GPO, Washington, D.C., 1949)].

tron capture between C^{+4} and He there are no appropriate final states. For double-electron capture from He by C^{+4} there is a number of excited states of C^{+2} as shown on Fig. 3(b) with appropriate energy defect. A similar situation exists for collisions between C^{+4} and Ne. For collisions between C^{+3} and Ne or Ar appropriate states exist in C^{+1} and C^{+2} to make single- or double-electron capture possible. For C^{+3} + He, double-electron capture would be endothermic, but single-electron capture can and does occur. In the case of C^{+4} collisions with Ar, single-electron capture can proceed to the $n=3$ states of C^{+3}, and this is consistent with the observation of a large cross section for this process. To satisfy the energy-defect criterion for double-electron capture from argon, either the C^{+2} produced can be in a doubly excited state or C^{+2} and Ar^{+2} can both be in excited states, and either of these is consistent with the observed cross section. As can be seen from Fig. 3, two-electron capture by C^{+5} is so exothermic that the C^{+3} would certainly be formed in a short-lived autoionizing state.[8] Since our detection method cannot presently distinguish C^{+4} ions generated by this process from those made by ordinary single-electron capture, this process may contribute to the measured cross section for single-electron capture by C^{+5}.

Theoretical calculations for these cross sections are in progress and work to determine the final states of products is underway.

The authors gratefully acknowledge useful discussions with Abraham Szöke and Norman Kurnit and skillful fabrication of the laser apparatus by the members of the Physics machine shop.

*Hertz Foundation Fellow.
†Present address: Department of Chemistry, Harvard University, Cambridge, Mass. 02138.

[1]D.R. Bates, H.C. Johnson, and I. Steward, Proc. Phys. Soc. London 84, 517 (1964).
[2]D.J. Rose and M. Clark, Jr., *Plasmas and Controlled Fusion* (M.I.T. Press, Cambridge, Mass., 1961), p. 33.
[3]For bibliography see R.A. McCorkle and J.M. Joyce, Phys. Rev. A 10, 903 (1974).
[4]J.B. Hasted and A.Y.J. Cheng, Proc. Phys. Soc. London 80, 441 (1962).
[5]H.J. Zwally and D.W. Koopman, Phys. Rev. A 2, 1851 (1970); see also, H.J. Zwally and P.G. Cable, Phys. Rev. A 4, 2301 (1971).
[6]J. Goldhar, Ph.D. thesis (M.I.T., Cambridge, Mass., 1976) (unpublished).
[7]H.J. Zwally, Rev. Sci. Instrum. 41, 1489 (1970).
[8]L.M. Kishinevskii and E.S. Perilis, Sov. Phys.-JETP 28, 1020 (1969).

APPENDIX C

Excimer

XeF ground-state dynamics in a laser discharge
Applied Physics Letters 33, 926 (1978).

XeF ground-state dissociation and vibrational equilibration
Applied Physics Letters 35, 247 (1979).

A Multilevel Model of XeF ground State kinetics - to be published.

XeF ground-state dynamics in a laser discharge[a)]

S. F. Fulghum, I. P. Herman,[b)] M. S. Feld, and A. Javan

Department of Physics and Spectroscopy Laboratory, Massachusetts Institute of Technology, Cambridge, Massachusetts 02139

(Received 7 July 1978; accepted for publication 25 September 1978)

The time evolution of gain and absorption in an XeF laser discharge is studied using a pulsed uv dye-laser probe and timing system with ±7-nsec resolution. The dissociation rate of the lowest vibrational level of the XeF ground state as a function of helium buffer pressure is found to have a slope of 1×10^{4} $sec^{-1}Torr^{-1}$ (±15%).

PACS numbers: 42.55.Hq, 82.30.Lp

The fact that the XeF ground electronic state is bound sets the XeF laser apart from the other rare-gas halide lasers in that its gain profile is inhomogeneously broadened, in contrast to the homogeneous broadening of KrF and ArF.[1] Therefore, energy-exchange processes among the vibrational levels of the XeF ground electronic state and the molecular dissociation rate are important factors in determining efficiency and energy extraction capabilities. This report studies the dissociation of XeF in a laser discharge by means of a pulsed-dye-laser probe technique with ±7-nsec time resolution. The measurements are based on the fact that the time-dependent absorption of certain XeF vibronic transitions is a direct indication of the decay of population in the XeF ground state.

The experiments use a tunable pulsed uv dye laser and timing system to probe the time evolution of gain/absorption on selected vibronic transitions in XeF formed in a laser discharge. The system consists of two photopreionized transverse discharge chambers with Blumlein-type excitation. These chambers are triggered independently with a relative delay which can be continuously varied. One (with mirrors) is used as a laser to pump a dye laser, whose output probes XeF formed in the second chamber. With appropriate optics and gas mixtures, this second chamber produces 25-mJ 20-nsec XeF laser pulses.

The relative delay between the dye laser probe and the XeF discharge is measured for each shot by a 100-MHz digital clock to eliminate errors due to jitter in the discharge timing. A fast photomultiplier with a uv filter starts the clock on the rising edge of fluorescence emitted from one end of the discharge. A separate photomultiplier samples the probe beam to stop the clock. The relative intensities of the dye-laser probe before (I_0) and after (I) the discharge chamber are determined by photomultipliers whose output currents are integrated and the resulting voltage digitized. This system allows measurement accuracy of ±3% in gain/absorption and ±7 nsec in time.

Pumping *p*-terphenyl, PPD, or PBD dyes with either a KrF or nitrogen laser provides 10–20-nsec pulses in the spectral range 3250–3620 Å. Well-separated vibronic bands have been probed from 4-1 [2,3] at 3350 Å to 0-5 at 3564 Å. [The notation 4-1 indicates a vibronic transition between the $v'=4$ vibrational level in the excited (B) state and $v''=1$ in the ground (X) state.] The spectral width of the dye-laser pulses is about 0.5 Å, narrow enough to fit within a particular band profile but broad enough to average over rotational structure. Photographic absorption spectra taken with a broadband dye laser are used to position the dye laser within a selected band. Band profile calculations with constants given by Tellinghuisen[4] and the absorption curves of Smith and Kobrinsky[5] are also used.

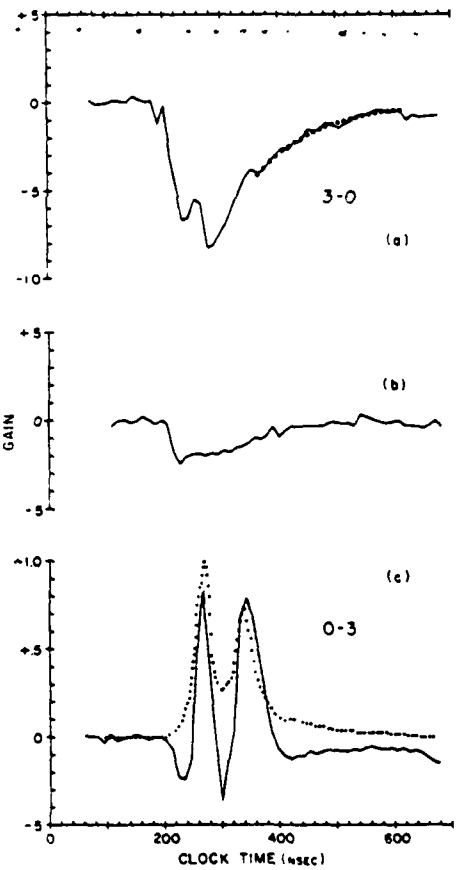

FIG. 1. Gain in a Xe, F_2, He laser discharge at 300 Torr: (a) XeF 3-0 transition (3359.8 Å). The dotted line is an exponential fit to the tail region. (b) Gain at 3359.8 Å with Xe removed from gas mixture (c) XeF 0-3 laser transition (3532.8 Å). The dotted line is 0-3 fluorescence. The double peaks are due to discharge current ringing.

[a)]Work supported by the Office of Naval Research.

[b)]Present address: Lawrence Livermore Laboratory, University of California, Livermore, Calif. 94550.

 0003-6951/78/3311-0926$00.50

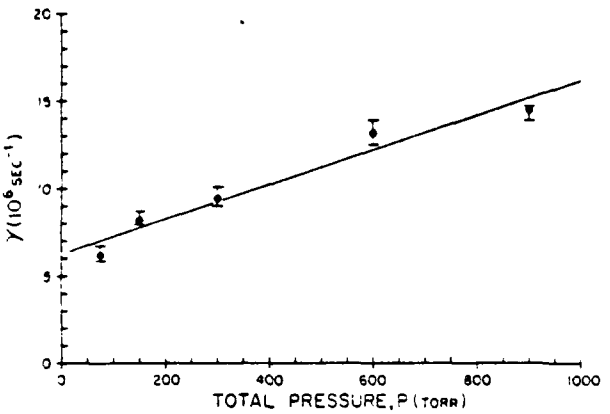

FIG. 2. Dissociation rate of the lowest vibrational level of the XeF ground state γ as a function of total pressure P, holding Xe and F_2 partial pressures fixed. The rates are obtained from fits such as that of Fig. 1(a).

A run consists of firing the lasers at 5—10-sec intervals while sweeping the relative probe delay back and forth over the region of interest until three or four absorptions have been recorded for each 10-nsec time slot. Shot-to-shot variations in the amount of XeF produced is the principal source of uncertainty. The standard deviation of the population difference, as calculated from the absorption, is typically no more than 15% of the mean. The apparent rise in the absorption in Figs. 1(a)—1(c) at very late times is due to scattering of the probe beam by arcs in the discharge. This makes the data less reliable at higher pressures, where the arching is more severe.

Figures 1(a)—1(c) plot gain as a function of time. For a weak probe the gain is given by $\ln(I/I_0)$, where I/I_0 is the measured probe-intensity ratio. The discharge length is 70 cm. The probe intensity is about 600 W/cm^2, below the saturation level for the conditions of the experiment. This is evidenced by the fact that I/I_0 remains the same for a particular delay when I_0 varies by a factor of up to 3 during a run.

Figure 1(a) shows the time evolution of the probe absorption with the dye laser centered at 3359.8 Å, the wavelength of the XeF 3-0 transition (B, $v'=3-X$, $v''=0$). The gas fill is 6 Torr Xe, 1.2 Torr F_2 with the balance He to a total pressure of 300 Torr. This absorption is a direct indication of the XeF ground-state population, since the population in the $v'=3$ level of the excited state is small in comparison to that of the $v''=0$ level in the ground state. Thus, the decay of the absorption in the tail region reflects the decay of XeF population in the $v''=0$ level.

Before discussing this curve, it is important to establish that the tail region is free from impurity absorption and that XeF excited-state production has ended. The solid curve in Fig. 1(c) is the result of probing one of the main laser transitions, 0-3, at 3532.2 Å in a discharge with an identical gas fill. (At pressures below about 450 Torr the gain has two peaks because of ringing in the discharge current.) The dotted curve is the corresponding 0-3 fluorescence. The fluorescence decay at ~380 nsec establishes that most of the excited-state production is completed prior to the tail region of the 3-0 absorption [Fig. 1(a)]. The regions of decreased absorption near the peak absorption in Fig. 1(a) are due to increased population in $v'=3$ and correspond to the gain peaks of Fig. 1(c).

Also, note that the gain curve of Fig. 1(c) shows an initial absorption signal, evidently due to an impurity, preceding the onset of XeF gain. To assess the extent of this impurity absorption similar curves were taken with one of the discharge constituents removed. Figure 1(b) probes a discharge mixture the same as that used above, but with the Xe removed. In this curve the dye laser is centered at the XeF 3-0 transition [same as Fig. 1(a)]. As can be seen, the initial absorption is the same as that of Fig. 1(c). Essentially identical initial absorptions in mixtures containing xenon were obtained at 3487 Å (2-5 transition), 3549 Å (0-4), and 3564 Å (0-5), as well as at wavelengths where XeF gain is small or absent (e.g., 3559 Å). This indicates that a broad-band absorber, possibly F^-,[6] is present in the laser discharge, and that the onset of this absorption precedes the XeF gain by about 50 nsec. However, Fig. 1(b) shows that this impurity absorption decays away and is small in the tail region of the 3-0 absorption.

Adding a trace amount of Xe to the discharge produces a weak fluorescence signal almost identical to that of Fig. 1(c), indicating that the discharge is not significantly affected by the removal of Xe. No absorption is detected in discharges of pure He or a He-Xe mixture.

Thus, we can conclude that the tail absorption of Fig. 1(a) is predominantly due to ground-state XeF.

The dotted line in Fig. 1(a) is an exponential least-squares fit to the tail region which gives the $v''=0$ decay rate γ at this pressure. Figure 2 shows how the observed rate varies as a function of the total pressure P when the partial pressures of Xe and F_2 are held at 6 and 1.2 Torr, respectively. The error bars reflect uncertainty in choosing the end points for the exponential fit, i.e., the beginning of the tail region and the point where the scattering effect sets in. A linear fit to these points gives

$$\gamma(P) = 6.3\times10^6 + (9.9\times10^3)P \text{ sec}^{-1} (\pm 15\%),$$

with P in Torr. Thus, the $v''=0$ decay rate due to helium is 1×10^4 sec^{-1} Torr^{-1}.

The Xe and F_2 background pressures, the unstable molecular species formed in the high-density plasma, and possibly cold electrons also contribute to the observed decay rate. They account for the residual rate extrapolated to zero helium pressure. Experiments that produce XeF from XeF_2 by photodissociation are in progress to determine dissociation rates in the absence of a discharge.

A recent parametric study of a similar laser discharge by Gower, Exberger, Rowly, and Billman[7] includes data on the transient absorption at 3336 Å, probed by an argon ion laser, which they tentatively assign entirely to F^-. We note that this line falls within the band profile of the XeF 4-0 transition,[5] similar to and slightly

ronger than the 3-0 transition we have used.[4] Therere, this data can be interpreted instead along the lines resented above. The reported[7] decay rate slope of 3×10^4 sec^{-1} Torr^{-1} with a He buffer is in agreement ith our result.

If vibrational equilibration within the ground state is ppreciably faster than the decay measured in our xperiments, then the vibrational-level populations apidly tend to a quasiequilibrium distribution. In this ase, the observed rate reflects the decay of this disibution, hence the decay of the ground state as a whole. , however, vibrational equilibration is incomplete, ien the observed rate primarily reflects the dissociaon of the $v''=0$ level. Preliminary results from the eF$_2$ photodissociation experiments on the decay of the $'=1$ level show a multiexponential decay with rates om $(1-3)\times10^4$ sec^{-1} Torr^{-1}, indicating only a partial quilibration.

Further experiments are necessary to determine the fetimes of the higher-lying vibrational levels, on which the main XeF laser transitions terminate, and the behavior of the XeF ground-state vibrational manifold as a whole.

Stimulating conversations with Mordechai Rokni and Larry Kline are gratefully acknowledged.

[1]J. Goldhar, J. Dickie, L.P. Bradley, and L.D. Pleasance, Appl. Phys. Lett. 31, 677 (1977).
[2]J. Tellinghuisen, G.C. Tisone, J.M. Hoffman, and A.K. Hays, J. Chem. Phys. 64, 4796 (1976).
[3]J. Tellinghuisen, P.C. Tellinghuisen, G.C. Tisone, J.M. Hoffman, and A.K. Hays, J. Chem. Phys. 68, 5187 (1978).
[4]P.C. Tellinghuisen, J. Tellinghuisen, J.A. Coxon, J.E. Velazco, and D.W. Setser, J. Chem. Phys. 68, 5177 (1978).
[5]A.L. Smith and P.C. Kobrinsky, J. Mol. Spectrosc. 69, 1 (1978).
[6]A. Mandl, Phys. Rev. A 3, 251 (1971).
[7]M.C. Gower, R. Exberger, P.D. Rowley, and K.W. Billman, Appl. Phys. Lett. 33, 65 (1978).

XeF ground-state dissociation and vibrational equilibration[a)]

S. F. Fulghum, M. S. Feld, and A. Javan
Department of Physics and Spectroscopy Laboratory, Massachusetts Institute of Technology, Cambridge, Massachusetts, 02139

(Received 30 April 1979; accepted for publication 29 May 1979)

The time evolution of the population in XeF ground-electronic-state vibrational levels is studied using a laser-induced fluorescence technique. The results indicate that a quasiequilibrium distribution is rapidly established within the vibrational manifold and that the dissociation rate of the molecular ground state as a whole is $(1.4\pm0.3)\times10^{4}\,\mathrm{sec}^{-1}\,\mathrm{Torr}.^{-1}$.

PACS numbers: 33.10.Gx, 34.50.Ez

The strongest XeF laser lines are B-X transitions which teminate on the $v''=2,3$, and 4 ground-state vibrational levels. In order to maintain laser oscillation, a population must be removed from these levels via collisions with the rare gas buffer. This occurs primarily by VT processes which redistribute the population among all the vibrational levels. Direct removal by collision-induced dissociation is less likely since the rotationless dissociation limit is about 3 kT above the levels in question. However, after molecules are transfered to higher-lying levels by vibrational and rotational thermalization, they are more easily dissociated. The overall dissociation proceeds primarily by such multistep processes.

The ground-state dynamics may be studied by monitoring the populations of the various vibrational levels. In an earlier experiment we measured the decay rate of the $v''=0$ level in a XeF laser discharge using an absorption technique.[1] The present studies extend these measurements to the $v''=1$ level using a laser-induced fluorescence technique in a passive low-pressure sample cell. The new technique has the advantages that the XeF is produced in a time very short compared to the overall decay rate, that the complications of a discharge are avoided, and that at low pressures the time scales of the relaxation processes are extended, making possible more precise measurements. The major finding, that the $v''=0$ and 1 decay rates are the same within experimental uncertainty, indicates that VT processes rapidly establish a quasiequilibrium within the vibrational manifold. The vibrational populations then decay away together at a single rate as molecules are dissociated from high-lying levels.

In the experiments XeF_2 vapor is placed in a 1-cm-long fused-silica fluorescence cell along with a buffer gas. The vapor pressure is held at 0.6 Torr by a 0 °C cold trap. A 20-nsec ArF laser pulse photodissociates the XeF_2 producing an initial XeF population, primarily in the excited B state. This XeF* rapidly decays via spontaneous emission, creating an initial ground-state population. After a measured delay, a 20-nsec pulse from a uv dye laser tuned to an appropriate B-X transition pumps molecules from a specific lower vibrational level back to the excited state. The amount of induced fluorescence thus produced is proportional to the population in the level at that time. Its intensity as a function of time delay gives the time evolution of the population in a given vibrational level.

The ArF and dye laser beams are irised and focused to a 3-mm diameter and overlap in the cell. The 1-mJ ArF pulses are weak enough to insure that the pressure of XeF and its dissociation products are small compared to the background pressure. The dye laser pulses have energies of about 20 μJ which is insufficient to saturate the weak transitions probed. The induced fluorescence is isolated from background fluorescence and scatter by a monochromator and then detected by a fast photomultiplier and oscilloscope. In analyzing the data, the induced fluorescence is normalized to the energies of both lasers for each shot.

The $v''=0$ and 1 levels are probed using the B-X 2-0 transition ($B,v'=2$; $X,v''=0$) at 3394 Å and the 2-1 transition at 3417 Å, respectively. In both cases fluorescence is observed on the relatively strong 2-5 transition at 3488 Å. The dye laser spectral width of $\frac{1}{2}$ Å fits easily into the band profiles but is wide enough to sample many rotational levels.

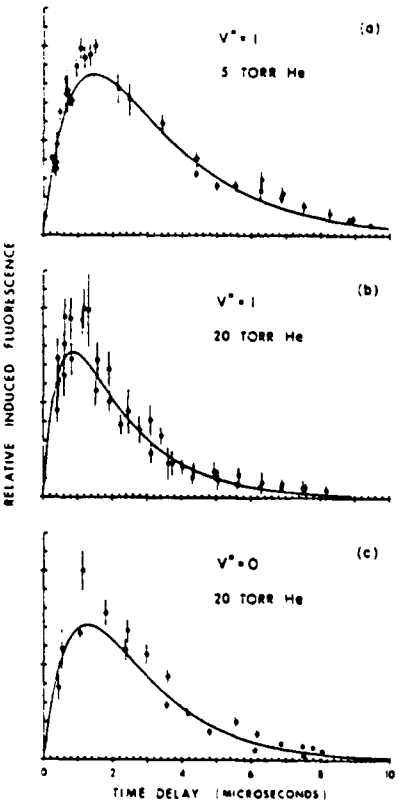

FIG. 1. XeF induced fluorescence intensity versus probe delay from XeF photodissociation. The XeF ground-state vibrational level being probed and the buffer gas pressure are as indicated.

a)Work supported by the Office of Naval Research.

 0003-6951/79/150247-03$00.50

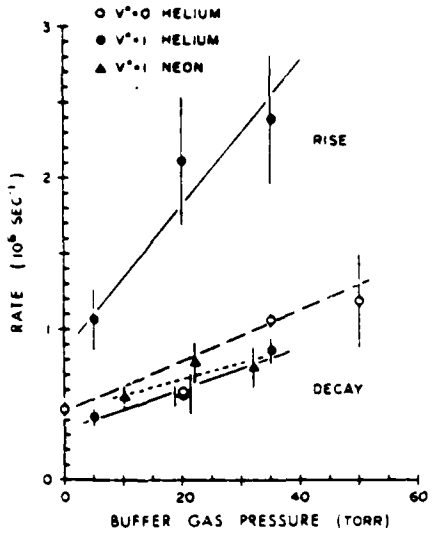

FIG. 2. Rates determined by two exponential fits such as in Fig. 1. The decay-rate–vs–pressure slopes are $v'' = 0$ with He, $1.68(\pm 0.15)\times 10^4$ sec^{-1} Torr^{-1}; $v'' = 1$ with He, $1.39(\pm 0.33)\times 10^4$ sec^{-1} Torr^{-1}; $v'' = 1$ with Ne, $1.08(\pm 0.65)\times 10^4$ sec^{-1} Torr^{-1}. The rise-rate–vs–pressure slope is $v'' = 1$ with He, $4.81(\pm 1.49)\times 10^4$ sec^{-1} Torr^{-1}.

Figures 1(a)–1(c) show data for levels $v'' = 0$ and 1 with a helium buffer. The error bars reflect uncertainties due to electrical noise, photomultiplier noise, and trace widths on the oscilloscope photographs. The general behavior is a rapid rise followed by a slower decay. The small initial values of the population are due to the fact that the largest Franck-Condon factors are for transitions which terminate on $v'' = 2,3$, and 4. The initial population, produced by the XeF* radiative decay is thus concentrated in these levels. The rise occurs as VT processes bring the vibrational manifold into equilibrium, transferring population to $v'' = 0$ and 1. The peak of the $v'' = 0$ curve roughly indicates when equilibration has occurred. The subsequent decay is due to the loss of molecules through dissociation, primarily from higher-lying vibrational levels.

The solid curves in Fig. 1 are fits to a two-exponential curve of the form $\exp(-\gamma_D) - \exp(-\gamma_R)$. The decay rate γ_D and the rise rate γ_R are plotted in Fig. 2 as functions of the buffer gas pressure. The slopes for the decay rates for $v'' = 0$ and 1 with a He buffer are the same to within experimental error, as is required by the existence of a quasiequilibrium. This value, $1.4(\pm 0.3)\times 10^4$ sec^{-1} Torr^{-1}, is in reasonable agreement with our earlier result of 1×10^4 sec^{-1} Torr^{-1} from the absorption experiments,[1] and somewhat faster than the rate of 6.4×10^4 sec^{-1} Torr^{-1} reported by Tang, Hunter, and Huestis for a He buffer.[2] It is also within the range of the theoretical predictions of Duzy and Shui[3] and Huestis.[4]

The decay rate for the $v'' = 1$ level using a neon buffer is essentially the same as the rate with a He buffer. This is consistent with other studies of collision-induced dissociation in diatomics, which show only a weak dependence on the mass of the third body.[5] Likewise, the VT rates in other diatomic systems have been shown to be relatively independent of the identity of the third body.[6]

The rising sections of the data are not well defined for most runs, particularly those at higher pressures. Only for the $v'' = 1$ runs with a He buffer could a significant slope of $(4.8 \pm 1.5)\times 10^4$ sec^{-1} Torr^{-1} be extracted (Fig. 2). This is probably an underestimate of the actual slope because the lack of points with short delays causes the fitting procedure to underestimate γ_R for the higher-pressure data. The $v'' = 1$ runs with Ne showed rise rate slopes close to those with He buffers and all runs on $v'' = 1$ had rise rate slopes greater than that of the $v'' = 0$ runs. A faster initial rise for $v'' = 1$ is expected since single quantum vibrational transitions are more likely than double quantum transitions, so that the population in $v'' = 0$ cannot build up significantly until the population in $v'' = 1$ has been established. It should be emphasized that a single exponential rise rate is only a means of characterizing the data. Preliminary results of a model which includes VT collisional mixing of all the ground-state vibrational levels makes it clear that the rise is composed of several rapid exponentials. The single rate should therefore be interpreted as a weighted average of the actual VT rates.

The simplest possible model of the XeF ground state (and the one used up to now in most laser simulations) employs a single level with an effective lifetime which is chosen to be consistent with steady-state laser behavior. To understand qualitatively how VT and dissociation processes determine this effective lifetime, consider a model in which the ground state consists of two levels, one representing the vibrational level on which laser emission terminates, and a second lower reservoir level which contains most of the equilibrium population. All the dissociation occurs from this reservoir level since it represents all the other levels in the ground-state vibrational manifold. Let the downward VT rate between the two levels be γ_{VT}, the reverse rate be $f\gamma_{VT}$, where $f < 1$ as determined by detailed balance, and the dissociation rate out of the lower level be γ_{dis}. In this model, the effective lifetime of the lower laser level is

$$\tau_{eff} = \gamma_{VT}^{-1} + f\gamma_{dis}^{-1}.$$

The first term is the effective lifetime when there is no population in the other ground-state levels. The second term represents the increase due to buildup of a population in the other vibrational levels and the resulting return flow into the lower laser level.

The rate γ_{dis} corresponds to the overall dissociation rate γ_D measured in our experiments. The rate γ_{VT} is related to the measured γ_R but should be several times faster since it primarily represents VT processes in higher vibrational levels. The detailed balanced factor can be roughly approximated by f for the levels $v'' = 3$ and $v'' = 0$ in XeF, which is $\simeq 0.07$. For a 1-atm He buffer this gives

$$\gamma_{VT}^{-1} < (4.8\times 10^4 \text{sec}^{-1}\ \text{Torr}^{-1} 760\ \text{Torr}^{-1}) = 27\ \text{nsec},$$

$$f\gamma_{dis}^{-1} = 0.07\ (1.4\times 10^4\ \text{sec}^{-1}\ \text{Torr}^{-1}\ 760\ \text{Torr}^{-1})$$
$$= 7\ \text{nsec}.$$

These numbers are consistent with effective lifetimes of 12–18 nsec atm, found by fitting single-level models to experimental data on XeF laser emission.[7,8] The estimate of τ_{eff} is

further reduced if direct dissociation out of the lower laser level is included.

The above model is only a first step in understanding the influence of VT and dissociation processes on XeF laser behavior. Development of a more general multilevel model is currently under way, along with experiments to determine improved VT parameters.

Useful comments from Larry Kline are gratefully acknowledged.

[1]S.F. Fulghum, I.P. Herman, M.S. Feld, and A. Javan, Appl. Phys. Lett. **33**, 926 (1978).
[2]K.Y. Tang, R.O. Hunter, and D.L. Huestis, presented at the 31st Gaseous Electronics Conf., Buffalo, New York, 1978 (unpublished).
[3]C. Duzy and V.H. Shui, see Ref. 2.
[4]D.L. Huestis, Stanford Research Institute Report No. MP 78-07, 1978.
[5]W.H. Wong and George Burns, J. Chem. Phys. **62**, 1712 (1975).
[6]M. Rubinson and J.I. Steinfeld, Chem. Phys. **4**, 467 (1974).
[7]M. Rokni, J.H. Jacobs, J.A. Mangano, and J.C. Hsia, see Ref. 2.
[8]T.G. Finn, L.J. Palumbo, and L.F. Champagne, Appl. Phys. Lett. **33**, 148 (1978).

249

A Multilevel Model of XeF Ground State Kinetics*

S.F. Fulghum†, M.S. Feld, and A. Javan

ABSTRACT

We present a multilevel model of energy transfer in the XeF ground electronic state due to collision-induced VT and dissociation processes. The model, whose parameters are based on experimental results presented here and on other recent data, should be useful in accurate simulations of output efficiency and multiline laser oscillation in XeF. Effective lifetimes of individual ground state levels, applicable to two level laser models, are determined from the multilevel model. The effective lifetime of the primary lower laser level, v"=3, is determined to be 4 to 6 nsec for a 1 atm He buffer.

*Work supported by NSF and in part by the Office of Naval Research

†Currently with Avco Everett Research Laboratory, Inc.

Introduction

In the early 1960's xenon was found to form stable compounds with fluorine, such as XeF_2, XeF_4, and XeF_6. The monohalide, XeF, however, was never isolated and was assumed to have a repulsive ground state. The emergence of rare gas monohalides as UV laser candidates in 1974 [1] again focused attention on XeF. The vibrational and rotational structure observed in laser fluorescence made it obvious that the transitions were bound-bound. This structure was analyzed by Tellinghuisen and co-workers, who determined that the ground state is indeed bound by about 1200 cm^{-1}, that it is highly anharmonic, and that it supports about 10 vibrational levels (Fig. 1).[2,3] The molecule is not stable in a practical sense because the shallow potential well allows rapid dissociation by collisional processes.

The efficiency of an XeF laser is limited by the rate at which these collisions with a buffer gas remove molecules from the relatively high lying levels on which the laser transitions terminate (v"=2,3,4). Population can be removed from these levels through collision-induced vibrational transitions (VT), collision-induced dissociation and by rotational equilibration, which can carry molecules to unstable rotational levels above the centrifugal barrier. Our aim has been to measure these rates directly and to estimate

their effects on XeF laser behavior. We will report our most recent measurements of the overall dissociation rate of XeF in a He buffer and the results of a model designed to extract VT and dissociation rates from the data. Such a multilevel model of the XeF ground state should be useful in laser simulations where accurate and detailed results are required.

Experimental Method

The method used is the technique reported previously in which XeF^* is produced by the photodissociation of XeF_2 with a 20 nsec ArF laser pulse.[4] This XeF^* rapidly decays via spontaneous emission, creating an initial nonequilibrium population distribution in the electronic ground state, primarily in levels v"= 2,3 and 4, since transitions terminating on these levels have the largest Franck-Condon factors.[3] After a measured delay, a 20 nsec pulse from a tunable UV dye laser, tuned to an appropriate B-X vibronic transition, probes a specific lower vibrational level. The fluorescence induced by the dye laser is proportional to the population in the level at that time. The rise of population in say v"=0, as population flows down from v"=2, 3 and 4, is a measure of the VT rates in XeF. The subsequent decay of this population, after a quasiequilibrium is established, is determined by both the VT rates and the direct dissociation rates out of individual levels. Figure 2 shows the buildup

and decay of population in v"=0 at various pressures of a He buffer. The tail of each set of points is well described by an exponential decay. Figure 3 plots these exponential decay rates versus pressure, along with a linear fit which gives the overall decay rate of a system in a quasiequilibrium.[4]

VT and Dissociation Rate Models

These experiments measure the net buildup and decay rates of population in a given level in the ground state. The problem is to extract from these measurements values for specific rates, such as the VT rate from v"=3 to v"=2 or the direct dissociation rate out of v"=3. Obviously, there are a great many such rates and to determine them individually from a few such measurements is not possible. The approach taken is to fit the experimental data with a model which expresses all of these rates with only a few parameters.

The overall model consists of two parts. One part describes the VT and dissociation rates of an XeF-buffer system and uses four parameters. These are the quantities required to estimate the effects of ground state kinetics on a laser system. The second part of the model describes effects particular to this experiment (and absent in a laser plasma) such as the background dissociation due to the XeF_2. The XeF-buffer system will be treated first.

The information theoretic approach of Procaccia and Levine is particularly well suited to expressing the VT rates in a convenient form.[5] It provides a set of "prior" VT rates using a single rate parameter and the known energy levels of the XeF molecule. Actual rates are then related to these prior rates in terms of the "surprisal", a measure of deviation. This surprisal parameter follows the well-known "exponential gap rule" which generally indicates that VT transitions involving large changes in vibrational energy have a lower probability of occurrence. Thus only two parameters need to be determined by the experiments to determine all of the VT rates. The specific form of the VT rate from v"=i to v"=j is taken to be:[5,6,7]

$$\hat{k}_{ji} = C_v \left[\frac{e^{\Delta} \Delta^2 K_2(\Delta)}{B_j} \right] e^{-2\lambda|\Delta|} , \qquad (1)$$

$$\Delta = (E_j - E_i)/2 ,$$

where E_i is the energy of the ith level, $K_2(\Delta)$ is the modified Bessel function of the second kind of order 2, B_j is the rotational constant of the final state and C_v and λ are the constants to be determined.

The overall dissociation of XeF is determined by these VT rates and by the direct dissociation rate out of each individual level. A variation of the Arrhenius equation is used to model these dissociation rates. It includes an

overall rate parameter and a vibrational bias parameter which allows for a dependence of the dissociation rate on the actual level of vibrational excitation. The form of the direct, collision-induced dissociation rate out of level v"=i, d_i, is thus taken to be:[8]

$$d_i = C_D e^{\frac{\beta E_i}{D_o}} e^{-(D_o - E_i)/kT}, \qquad (2)$$

where E_i is the energy of the vibrational level at the peak of its rotational manifold (J=24), D_o is the peak of the centrifugal barrier for J=24 and C_D and β are the constants to be determined.

The following set of equations uses the above rates to describe the relaxation of the vibrational level populations, N_i, in an XeF-buffer system.

$$\dot{N}_i = -d_i N_i + \sum_{j \neq i} \left(k_{ij} N_j - k_{ji} N_i \right) \qquad (3)$$

Note that once the rate constants are determined by a room temperature experiment, Eqs. (1) and (2) allow extrapolation to higher temperatures.

To limit the number of parameters to be varied in the fits we have fixed λ and C_D. Rubinson and Steinfeld have analyzed their extensive data on inelastic collisions of I_2^*

with rare gas atoms and find that this data is well described by the surprisal model with λ in the range of 2.5 to 4.5.[6] An early calculation by Huestis used the data of Refs. 6 and 9 and the exponential gap representation with $\lambda \cong 3$ to estimate the role of VT rates and collisional dissociation on XeF laser behavior.[10] Theoretical calculations by Duzy and Shui, which use a combination of phase-space theory and semi-classical trajectory calculations, indicate that λ for XeF and a Ne buffer is between 2 and 3.[11] We choose $\lambda = 3$ for our analysis.

For a given β the overall dissociation rate parameter C_D can be fixed by assuming that molecules in vibrational states at the dissociation limit will dissociate at the gas kinetic rate, which is taken to be 3×10^{-10} cm^3 sec^{-1}. In addition, since the peak of the rotational manifold (J=24) in levels v"=8 and 9 is above the centrifugal barrier, these levels are presumed to dissociate at the gas kinetic rate and reverse processes from these levels are set equal to zero.

As mentioned previously, in fitting our data two additional parameters are introduced to describe the effects of XeF_2. (These parameters are not used for laser modeling.) Even though we work at relatively low pressures of XeF_2 compared to He, XeF_2 is still effective in dissociating XeF. This effect can be seen in Fig. 3, which shows a background

rate, primarily due to the XeF_2. In the experimental fits this background rate is modeled by a single overall exponential decay. The fits to the v"=0 data (Fig. 2) use a background rate of 4.5×10^5 sec^{-1}. The v"=1 data reported previously [4] (Fig. 4) show a somewhat lower background rate and are fit with a 2.5×10^5 sec^{-1} overall rate.

Another effect due to the XeF_2 is a mixing of the two lowest vibrational levels. Figure 4 shows the buildup and decay of population in v"=1 at 5 and 20 Torr of He. Although the v"=1 data rises somewhat faster than that of v"=0, Eq. (3) predicts an even faster rise rate and a sharper peak for v"=1. This suggests that, in the experiment, the two levels are closely coupled, possibly by the near resonance between the ν_2 bending mode of XeF_2 (212 cm^{-1}) [12] and the 0-1 vibrational transition of XeF (204 ± 4 cm^{-1}). [3] To simulate this effect a mixing rate of 1.5×10^6 sec^{-1} is included in the model between levels 0 and 1, which is approximately the gas kinetic rate for collisions between XeF and XeF_2.

To establish that the background rate is, in fact, primarily due to XeF_2, additional data was taken at a reduced XeF_2 pressure. By lowering the temperature of the cold finger containing the solid XeF_2 from 0 °C to -18 °C, the vapor pressure was reduced by a factor of 6 to 0.1 Torr. Figure 5 shows data for v"=0 with 10 Torr of He. The solid curve is

the result of the model using the parameters from the 0 °C fit (described below) except that the background rate and the 0-1 mixing rate are reduced by a factor of 6. Although the data is noisy, it clearly indicates that the XeF_2 is the primary cause of the background dissociation.

Fit to Experimental Data

These rates are incorporated into a 10-level model of the ground state (Eq. 3 with XeF_2 terms added), which can be solved using numerical matrix methods. The initial population is assumed to be equally distributed among levels v"=2,3 and 4 since the Franck-Condon factors into these levels dominate and are roughly equal [3]. The results are not very sensitive to the particular distribution assumed among these higher levels. The negative eigenvalue of the rate matrix with the smallest absolute value is the overall decay rate of the system in a quasiequilibrium. This overall decay has been measured both by two exponential fits [4] to the new data (Fig. 3) and by previous absorption experiments. [13] The minimum eigenvalue is typically about ten times smaller than the next, giving an unambiguous overall decay rate. The positive exponentials, however, are typically quite close together, so that no individual rate can characterize the rising portion of the data. This model was fit to the data in Fig. 2 by adjusting the two free parameters until the peaks were matched as

closely as possible, while maintaining a minimum eigenvalue close to the measured overall decay rate. The solid curves in Fig. 2 are plots of the final fit using the buffer gas pressure as the final parameter. The primary parameters used in the fit are:

$$C_V = 1.0\times10^{-12}\ \text{cm}^2\ \text{sec}^{-1} \qquad \lambda = 3$$
$$C_D = 6.1\times10^{-12}\ \text{cm}^3\ \text{sec}^{-1} \qquad \beta = 3.9 \tag{4}$$

with the background rate set at $4.5\times10^{5}\ \text{sec}^{-1}$ and the 0-1 mixing rate at $1.5\times10^{6}\ \text{sec}^{-1}$.

These results indicate that, with regard to the removal of population from levels v"=2,3 and 4, direct dissociation is as effective or more effective than vibrational relaxation. Direct dissociation can be faster than VT processes because it includes both vibrational and rotational energy transfer.

XeF laser behavior can be modeled by supplementing Eqs. (1)-(3) and the parameters of Eq. (4) with similar rate equations for at least two upper laser levels, laser pumping terms, source terms and equations for the output intensities. Such a model is essential for the accurate estimation of energy extraction efficiency, and for describing multilevel processes such as bottlenecking and competition between the three primary transitions, 0-2, 0-3 and 1-4 (Fig. 1).

Specific examples of laser modeling of this type can be found in Ref. 7.

Effective Lifetimes

The multilevel model described above may be unnecessarily complex for some applications. If only the primary transition, 0-3, needs to be modeled, a two level model may give fairly accurate results. In this limit the ground state vibrational manifold is represented by a single level which decays with an effective lifetime, τ . This lifetime relates the steady state population, N_L° , in the lower level to the rate of supply of population, Λ , into that level, due to both stimulated and spontaneous emission:

$$N_L^\circ = \tau \Lambda . \tag{5}$$

In this case the effective lifetime is simply the inverse of the total dissociation rate out of the lower level. For the two level laser model such quantities as laser extraction efficiency and output power are proportional to

$$1 - \frac{\tau}{\tau_R} , \tag{6}$$

where τ_R is the radiative lifetime of the upper laser level.[7]

This simple effective lifetime can be related to the multilevel model and experimental parameters described above. In a multilevel system a rate into any one level results in population flowing into neighboring levels also, so that relating the steady state populations to the constant rates into each level requires a matrix. This effective lifetime matrix can be determined numerically, column by column, by introducing a unit source term into that particular vibrational level in Eq. (3). The resulting steady state populations are the elements of this lifetime matrix. We find that the diagonal elements dominate, which means that, to a good approximation, the simple definition of an effective lifetime is applicable to the higher levels such as v"=2,3 and 4. For equal rates into these three levels, the equilibrium populations predicted by the model using the parameters of Eq. (4) gives

$$\tau(4) = 1.5, \quad \tau(3) = 4.5, \quad \tau(2) = 12.2 \text{ nsec atm}, \tag{7}$$

where $\tau(v")$ denotes the effective lifetime of the v" level. Since 0-3 is the primary lasing transition at room temperature, the value of $\tau(3)$ would be the effective lifetime most appropriate to use in a two level model of the XeF laser. Comparisons between two level laser models and laser models with a ten level ground state vibrational manifold show good agreement for laser efficiency if a 4 nsec

effective lifetime is used in the two level case.[7] This indicates [Eq. (6)] that the finite lifetime of the lower laser levels decreases the laser extraction efficiency by about 30% at one atmosphere, in reasonable agreement with calculations based on the multilevel model. These lifetimes, in themselves, do not preclude steady state or long pulse lasing at one atmosphere.

Effect of Increased Temperature

There is considerable interest in the increased efficiency of XeF lasers run at elevated temperatures.[14] Our models of the VT rates and direct dissociation rates [Eqs. (1),(2)] can be used to extrapolate our room temperature measurements of these rates to elevated temperatures. At 450 °C, this gives:

$$\tau_{450}(4) = 0.5, \quad \tau_{450}(3) = 1.2, \quad \tau_{450}(2) = 2.6 \text{ nsec amagat.} \quad (8)$$

Thus, raising the temperature to 450 °C should increase the extraction efficiency by about 20%, at least insofar as the effects of increased VT and dissociation rates are concerned. Since the observed increase in efficiency is about a factor of two[14], most of the increased efficiency should be due to other processes, such as a decrease in absorption at higher temperatures.[15] The multilevel model can be used for

detailed predictions of the relative intensities of the laser emission at the primary transitions under these conditions.[7]

Error Estimate

Finally, the question of the probable error in these measurements and models must be addressed. The overall dissociation rate is fairly well defined now by the two different types of experiments we have performed.[4,13] The value of $9.9(\pm 2.5)\times10^{3}$ sec^{-1} $Torr^{-1}$ is not dependent on the details of the model we have chosen to represent the equilibration and dissociation of the ground state. The VT rate and dissociation rate parameters are not as well defined. This is due to the difficulty of fitting exponential curves of this form and the limited data that we have in the rising portion of the data sets.

In general, the model fits the data quite well at 10, 25 and 45 Torr of He, where the expected rise times are not too fast. The curve at 95 Torr, however, shows that either the experiment cannot properly measure rise times of less than about 300 nsec or that other kinetic processes not considered in the model occur which slow the rise rate immediately after the photodissocation of the XeF_2. The same effect is seen in the v"=1 data at 20 Torr, where the rise time is again predicted to be faster. This is possibly an effect of the

XeF_2 background.

A good way to indicate the practical effects of possible errors in the parameters is to show how they change the simple effective lifetimes. The assumption of a mixing rate between v"=0 and 1 increases the rise time of the v"=0 population in the model, which must be offset by a decrease in C_v to fit the peaks. Thus the C_v parameter determined by the fits could be low by a factor of two or possibly three. Using a C_v of 3×10^{-12} cm^2 sec^{-1} and decreasing the direct dissociation rates to maintain the same overall dissociation rate gives

$$\tau'(4) = 1.9, \quad \tau'(3) = 6.1, \quad \tau'(2) = 15.8 \text{ nsec atm}, \tag{9}$$

which are reasonably close to the results of Eqs. (7). This is not surprising, since the effective lifetime of a level, neglecting the return flow of population from neighboring levels, is approximately

$$(\gamma_v + \gamma_d)^{-1} \tag{10}$$

where γ_v is the total VT rate out of the level and γ_d is the direct dissociation rate out of the level.[7] Increasing one while decreasing the other tends to leave their sum unchanged.

The overall decay rate from the experimental fit (in the absence of XeF_2) is 8.25×10^3 sec^{-1} $Torr^{-1}$. Assuming a faster rate of 1×10^4 sec^{-1} $Torr^{-1}$ gives $\tau'(3) = 3.9$ nsec atm, while a slower rate of 6.5×10^3 sec^{-1} $Torr^{-1}$ gives $\tau'(3) = 5.4$ nsec atm. Assuming $\lambda = 2$ instead of 3 while maintaining a constant VT rate from v"=0 to 1 (to maintain the peak positions) only changes $\tau'(3)$ to 4.6 nsec atm. The effective lifetime of the primary lower laser level, v"=3, is thus within the range of 4 to 6 nsec atm.

Summary

In conclusion, we have developed a multilevel model of the XeF ground electronic state vibrational manifold which includes dissociation and vibrational equilibration rates. This model has been fit to experimental data to derive rate parameters which can be used for accurate estimates of XeF laser extraction efficiency and for modeling aspects of laser behavior involving more than one transition. Effective lifetimes for individual levels are derived which can be used in simpler two level laser models. The temperature dependence predicted by these models should prove useful in determining conditions under which laser efficiency is optimized.

REFERENCES

(1) J.E. Velazco and D.W. Setser, "Bound-free emission spectra of diatomic xenon halides," J. Chem. Phys., vol. 62, pp. 1990-1991, 1975

(2) J. Tellinghuisen, P.C. Tellinghuisen, G.C. Tisone, J.M. Hoffman, and H.K Hayes, "Spectroscopic studies of diatomic noble gas halides. III Analysis of XeF 3500 Å band system," J. Chem. Phys., vol. 68, pp. 5177-5186, 1978

(3) P.C. Tellinghuisen, J. Tellinghuisen, J.A. Coxon, J.E. Velazco, and D.W. Setser, "Spectroscopic studies of diatomic noble gas halides. IV Vibrational and rotational constants for the X,B and D states of XeF," J. Chem. Phys., vol. 68, pp. 5187-5198, 1978

(4) S.F. Fulghum, M.S. Feld, and A. Javan "XeF ground state dissociation and vibrational equilibration," Appl. Phys. Lett., vol. 35, pp. 247-249, 1979

(5) I. Procaccia and R.D. Levine, "Vibrational energy transfer in molecular collisions: An information theoretic analysis and synthesis," J. Chem. Phys., vol. 63, pp. 4261-4279, 1975

(6) M. Rubinson and J.I. Steinfeld, "Entropy analysis of product energy distributions in nonreactive inelastic collisions," Chem. Phys., vol. 4, pp. 467-475, 1974

(7) S.F. Fulghum, Ph.D. thesis, M.I.T., 1980 (unpublished)

(8) J.H. Kiefer, H.P.G. Joosten, and W.D. Breshears, "On the preference for vibrational energy in diatomic dissociation," Chem. Phys. Lett., vol. 30, pp. 424-428, 1975

(9) R.B. Kurzel and J.I. Steinfeld, "Energy-transfer processes in monochromatically excited iodine molecules. III Quenching and multiquantum transfer from v'=43," J. Chem. Phys., vol. 53, pp.3293-3303, 1970

(10) D.L. Huestis, R.M. Hill, D.J. Eckstrom, M.V. McCusker, D.C. Lorents, H.H. Nakano, B.E. Perry, J.A. Margevicius, and N.E. Schlotter, "New electronic transition laser systems," SRI International Technical Report No. MP 78-07, pp. 113-118, May 1978

(11) C. Duzy, private communication

(12) U. Nielsen and W.H.E. Schwarz, "VUV spectra of the xenon fluorides," Chem. Phys., vol. 13, pp. 195-202, 1976

(13) S.F. Fulghum, I.P. Herman, M.S. Feld, and A. Javan, "XeF ground-state dynamics in a laser discharge," Appl. Phys. Lett., vol. 33, pp. 926-928, 1978

(14) J.C. Hsia, J.A. Mangano, J.H. Jacob, and M. Rokni, "Improvement in XeF laser efficiency at elevated temperatures," Appl. Phys. Lett., vol. 34, pp. 208-210, 1979

(15) L.F. Champagne, "Temperature-dependent absorption processes in the XeF laser," Appl. Phys. Lett., vol. 35, pp. 516-519, 1979

FIGURES

Fig. 1. XeF B and X state vibrational levels and primary laser transitions.

Fig. 2. Net buildup and decay of population in v"=0 with a He buffer as indicated by induced fluorescence. XeF_2 at 0.6 Torr. Solid curve is the multilevel model fit.

Fig. 3. Decay rate of population in v"=0 from data in Fig. 1 (dots) compared to data published previously in Ref. 4 (crosses). Slope of linear fit is 9.9×10^3 sec^{-1} $Torr^{-1}$.

Fig. 4. Population in v"=1 with a He buffer and XeF_2 at 0.6 Torr. Solid curve is the multilevel model fit.

Fig. 5. Population in v"=0 with a He buffer and XeF_2 at 0.1 Torr. Solid curve is the multilevel model fit.

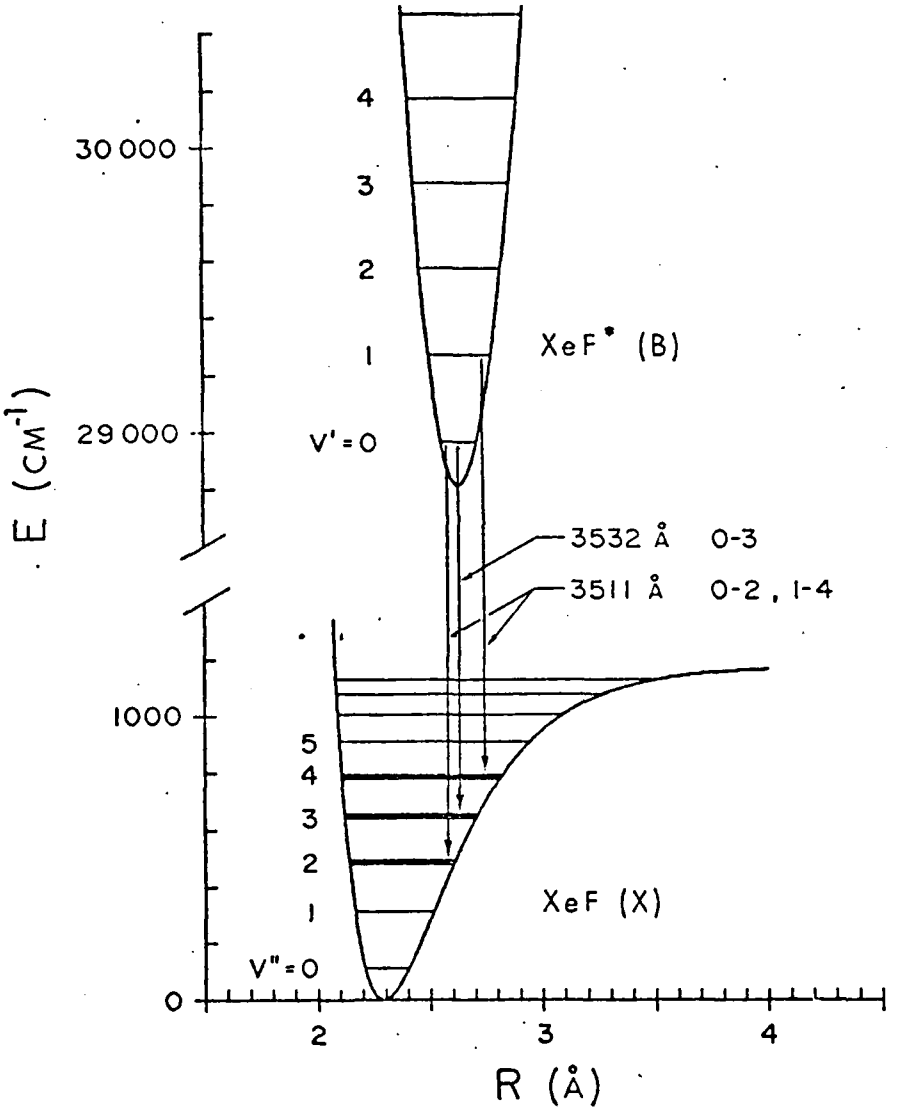
E (CM⁻¹)
30 000
29 000
1000
0
4
3
2
1
V' = 0
XeF* (B)
3532 Å 0-3
3511 Å 0-2, 1-4
5
4
3
2
1
V" = 0
XeF (X)
2
3
4
R (Å)

FIGURE 1

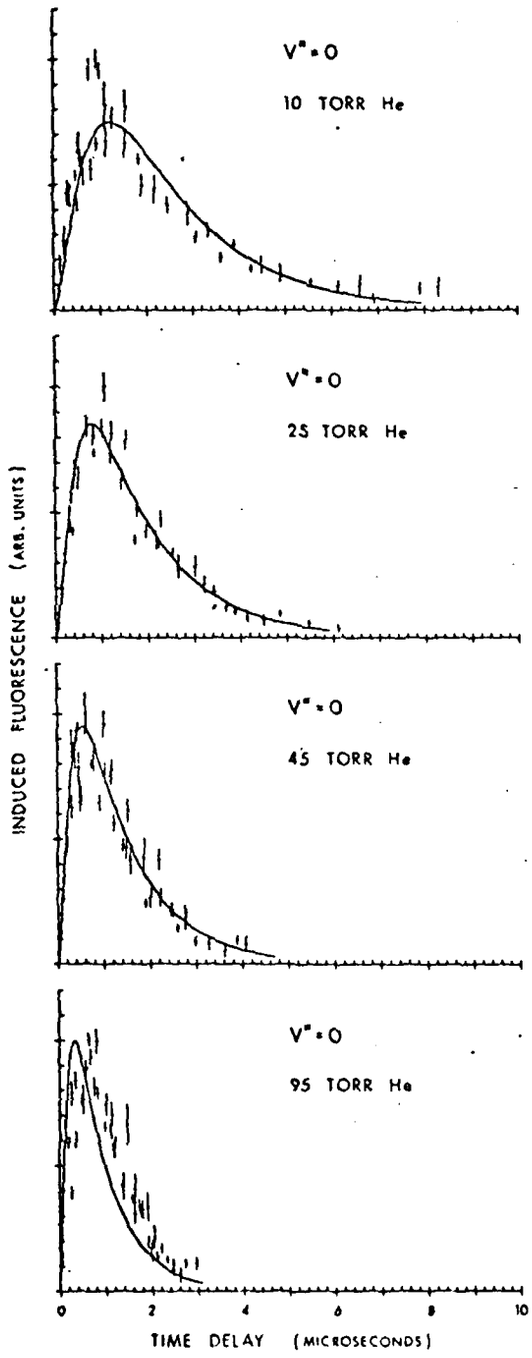
V"=0
10 TORR He
V"=0
25 TORR He
V"=0
45 TORR He
V"=0
95 TORR He
INDUCED FLUORESCENCE (ARB. UNITS)
0
2
4
6
8
10
TIME DELAY (MICROSECONDS)

FIGURE 2

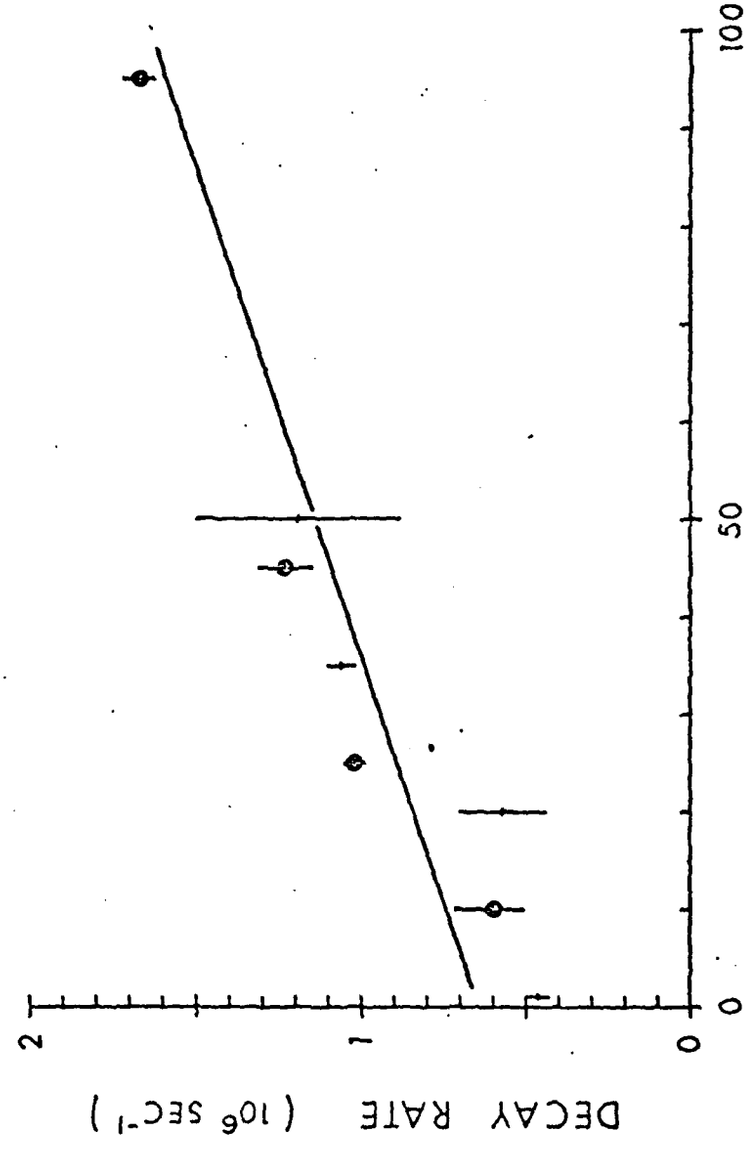

FIGURE 3

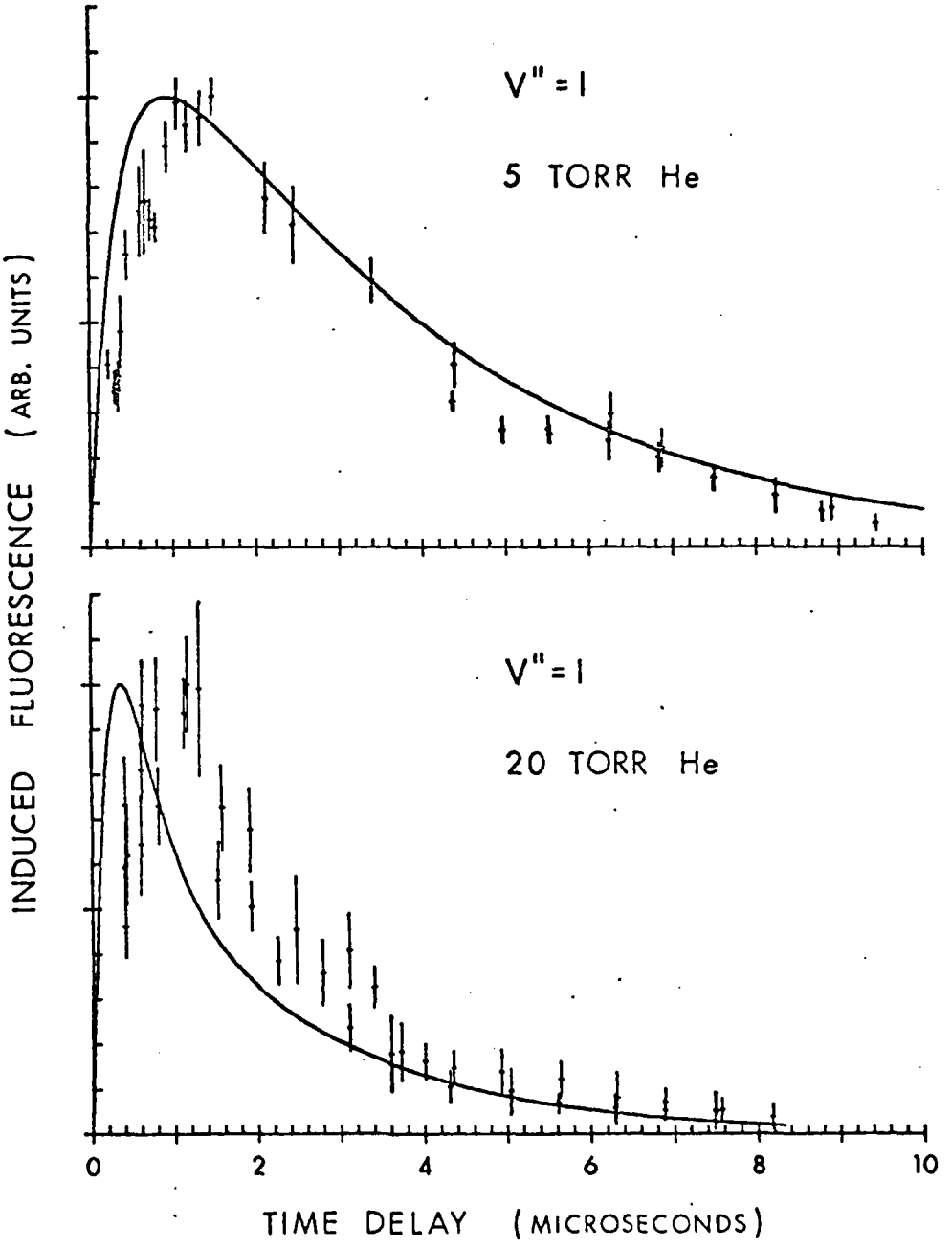
V" = 1
5 TORR He
V" = 1
20 TORR He
INDUCED FLUORESCENCE (ARB. UNITS)
0
2
4
6
8
10
TIME DELAY (MICROSECONDS)

FIGURE 4

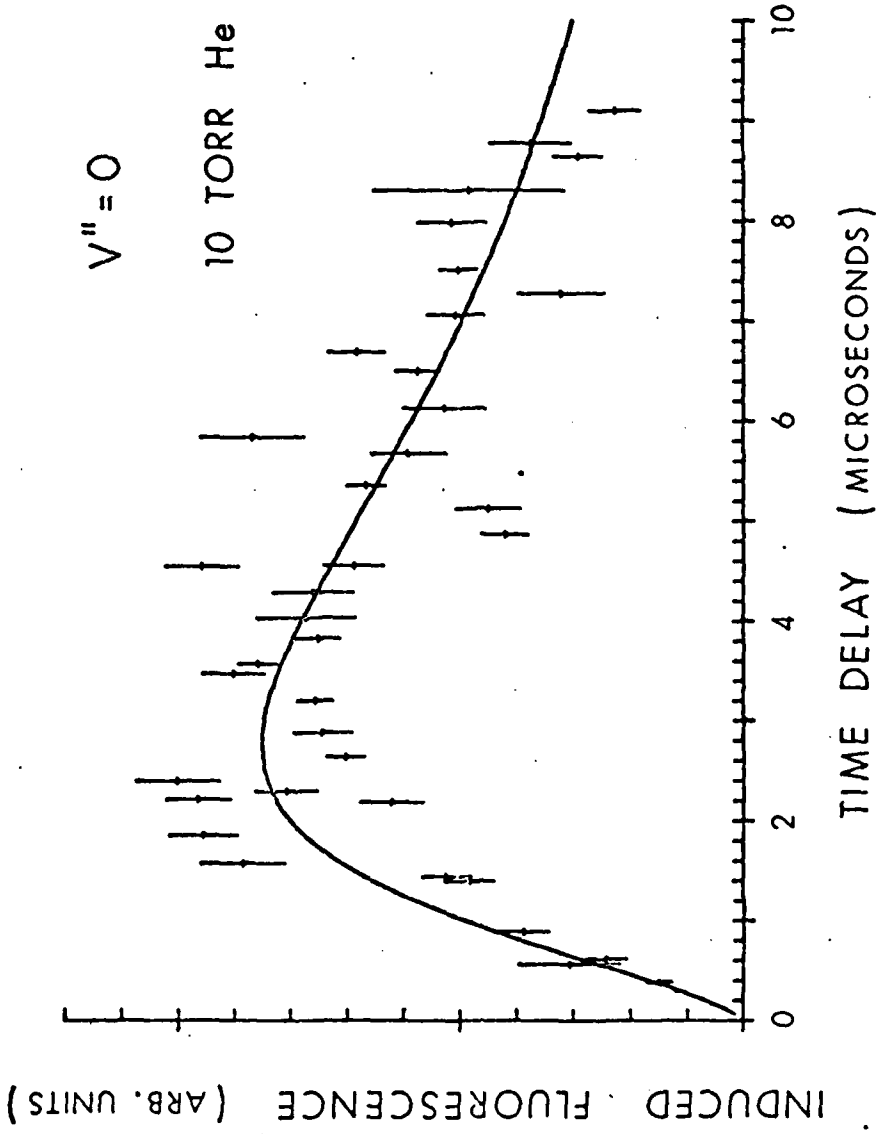
V"=0
10 TORR He
INDUCED FLUORESCENCE (ARB. UNITS)
TIME DELAY (MICROSECONDS)
0
2
4
6
8
10

FIGURE 5

APPENDIX D

Photopreionization

Photopreionization of the 3371-Å Pulsed N_2 Laser
IEEE Journal of Quantum Electronics, QE-11, 174 (1975).

Sealed multiatmosphere CO_2 TEA laser: Seed-gas compatible system using unheated oxide catalyst
Applied Physics Letters 32, 726 (1978).

Photopreionization of the 3371-Å Pulsed N_2 Laser

N. A. KURNIT, S. J. TUBBS, K. BIDHICHAND, L. W. RYAN, JR., AND A. JAVAN

Abstract—Photopreionization of the 3371-Å pulsed N_2 laser by use of a seed gas of low ionization threshold and flashlamp excitation is observed to result in increased laser output and reproducibility. Preionization also increases the range of permissible operating pressures, enabling operation with atmospheric-pressure mixtures of N_2 and He without reduced intensity.

The 3371-Å pulsed N_2 laser [1] requires large current densities ($\gtrsim 1$ kA/cm^2) and high electron temperature ($\gtrsim 5$ eV) [2]. In order to operate with sufficiently high E/p to achieve these values, the N_2 laser is typically operated in a transverse discharge configuration with electric fields of ~10–30 kV/cm and pressure of 30–100 torr [3]. At higher pressures [4], where large amounts of energy could be stored and extracted, nonuniformities in the discharge leading to the formation of arcs tend to degrade the laser performance.

We have investigated the effect of volume photopreionization on the nitrogen-laser performance using a seed gas of low photoionization threshold and an external flashlamp [5]. The seed gas is used at sufficiently low partial pressure to ensure that the electron temperature is largely dominated by collisions with N_2 molecules. We observe significantly improved discharge uniformity and suppression of arcs over a wide pressure range, improved reproducibility of both the spatial distribution and intensity of the laser output, some increase in permissible operating pressures, including the ability to operate with atmospheric-pressure mixtures of N_2 and He, and an

Manuscript received December 13, 1974. This work was supported by the Office of Naval Research and the Air Force Cambridge Research Laboratories.

N. A. Kurnit, K. BidhiChand, L. W. Ryan, Jr., and A. Javan are with the Department of Physics, Massachusetts Institute of Technology, Cambridge, Mass. 02139.

S. J. Tubbs is with the Department of Meteorology, Massachusetts Institute of Technology, Cambridge, Mass. 02139.

 Annals No. 504QE011

increase in average laser power. The method also allows the use of a large-volume N_2 plasma (which requires excitation at correspondingly higher total current). This is of importance in possible realization of a high-energy N_2 laser.[1]

In the experiments, the nitrogen laser was similar to a design described by Small and Ashari [6] in which the current pulse is produced by a flat-plate Blumlein circuit consisting of two 25 X 25-cm capacitors etched on 18-mil-thick double-clad epoxy circuit board and charged to typically 16 kV. The electrodes are 10-mil-thick copper strips soldered along the length of the capacitors and edge opposed inside an evacuable lucite box. Electrode spacings of 1 cm and 0.2 cm have been tested. A single mirror was used at one end of the laser. Since the discharge is pressure confined in this laser, rather than confined by dielectric walls as in a number of designs, it is possible to place a standard Xe flashlamp inside the lucite box adjacent to the discharge region. We have utilized a 35-cm-long flashlamp placed 1.5 cm from the discharge and pulsed with typically 1.5 J (0.01 μF charged to 17 kV) in $\sim$5 μs. The volume preionization is produced by addition of trace amounts of triethylamine $[(C_2H_5)_3N]$ in a manner similar to that reported earlier for the production of large-volume high-density CO_2-laser plasmas [7]. The flashlamp current pulse is used to trigger a spark gap which initiates the laser discharge after a variable delay of 15–100 μs. The purpose of the photopreionization in this application is only to provide a sufficiently uniform initial electron distribution to ensure the creation of a uniform plasma when a voltage above avalanche breakdown is applied across the laser electrodes, and hence delay arc formation beyond the time during which laser oscillation occurs; thus only a small fraction of the total electron density need be supplied by the photoionization.

Before the introduction of triethylamine into the laser medium, it was observed that pulsing the flashlamp had little or no effect on the laser characteristics. For pure N_2 at low pressures ($\sim$100 torr), addition of small amounts of seedant by bubbling a small percentage of the laser gas through liquid triethylamine was, even without the flashlamp, sufficient to give a significant improvement in discharge uniformity and as much as a factor-of-2 increase in output power, to $\sim$50 kW in a 4-ns pulse.[2] The flashlamp gave a further small increase in laser power and reproducibility.[3] Fig. 1(a) shows a plot of relative laser output energy as a function of N_2 pressure both with and without preionization, for a 1-cm-wide discharge. The most significant visual differences occur on the high-pressure side of the curve, where the output without preionization becomes strongly arc limited.

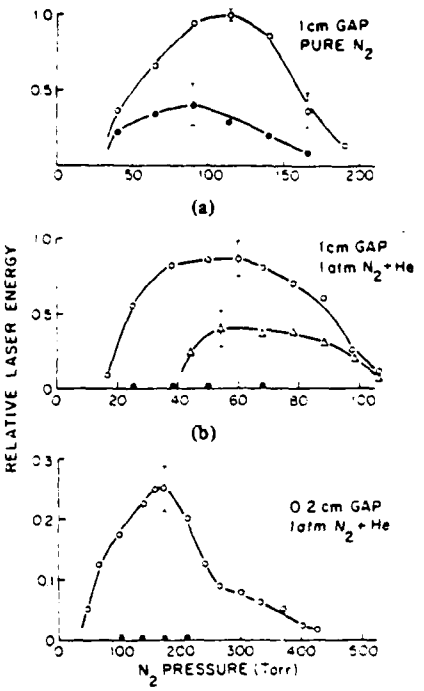

Fig. 1. Relative laser energy as a function of N_2 pressure for a) pure N_2 in 1-cm-gap laser, b) atmospheric-pressure mixture of N_2 and He with 1-cm gap, and c) atmospheric-pressure mixture of N_2 and He in 0.2-cm-gap laser. Open circles give output with flashlamp and optimized triethylamine flow; dots show output with no flashlamp and with triethylamine thoroughly purged from system. With atmospheric-pressure mixtures there is negligible output in the latter case. Triangles in (b) show output with triethylamine alone. Error bars indicate typical range of fluctuations during a series of 10 consecutive shots. (Magnitude of fluctuations is relatively constant along most curves, with corresponding decrease in percentage fluctuations near the peak of the curve; in the optimized curve in (a), a further decrease in fluctuations is observed near the peak of the curve.) Note the difference in pressure scales; in particular, (b) and (c) are scaled for the same ratio of field strength to nitrogen partial pressure.

A more dramatic behavior is illustrated in Fig. 1(b), which shows the laser output for an atmospheric-pressure mixture of N_2 and a He buffer[4] as a function of N_2 partial pressure, as determined from relative flow rates. Here, with no preionization the current is concentrated in a few arcs and there is negligible laser output, whereas with preionization the output is close to that obtained with pure N_2.

In this case again, triethylamine itself helps to produce a discharge which gives some laser action, but the laser performance is greatly improved when the flashlamp is fired shortly before the laser discharge. Delays of more than 50 μs between the flashlamp and laser reduce the effectiveness of the preionization. The discharge takes the form of a uniform distribution of closely spaced streamers as reported in [4], where atmospheric-pressure operation with pure N_2 was reported

[1] A publication which has just appeared in print discusses a different method in which a photostabilized discharge without the use of a seed gas is used to improve the performance of a UV N_2 laser; see V. Hasson, D. Preussler, J. Klimek, and H. M. von Bergmann, "Transverse double-discharge high-pressure glow excitation of UV lasing action in molecular nitrogen," *Appl. Phys. Lett.*, vol. 25, pp. 654–656, 1974.

[2] This effect may be attributable to the rapid rate of electron production from the low ionization threshold impurity. A similar effect has been reported in a CO_2–N_2–He laser mixture; see R. L. Schriever, "Uniform direct-current discharges in atmospheric-pressure He/N_2/CO_2 mixture using gas additives," *Appl. Phys. Lett.*, vol. 20, pp. 354–356, 1972. The laser power is strongly dependent on the fraction of volume utilized, the current density and rise time, and on whether the double-pass gain is high enough to saturate the transition.

[3] These experiments were performed at sufficiently low repetition rates ($\sim$2 pulses per second) so that the gas has time to be exchanged between shots. Some increase in reproducibility in such lasers can sometimes be observed at higher repetition rates, presumably due to some remaining background ionization, but for large energy deposition and high repetition rates arcing occurs if the gas is not exchanged quickly enough; see, for example, R. Targ, "Pulse nitrogen laser at high repetition rate," *IEEE J. Quantum Electron.* (Corresp.), vol. QE-8, pp. 726–728, Aug. 1972.

[4] T. Kobayasi, M. Takemura, H. Shimizu, and H. Inaba have reported such operation ("TEA UV nitrogen laser and its application to high sensitivity remote pulsed-Raman spectroscopy of atmospheric pollutants," presented at the IQEC 7th Int. Quantum Electronics Conf., Montreal, P. Q., Canada, May 1972, Paper M.9), but only at higher field strengths and with reduced intensity.

using higher field strengths and faster dielectric switches. It appears that photoionization should help to stabilize the discharge in such a TEA laser. The ability to operate at atmospheric-pressure mixtures of N_2 and He may in itself prove to be useful for some applications.

The maximum applied voltage of 16 kV was limited in these experiments by the breakdown potential of the epoxy board. In order to test the laser performance at higher E/p, a similar laser with a 2-mm gap was constructed. In this laser, with no photopreionization, the discharge was arc dominated at all but the lowest pressures, and laser performance was very poor. Photopreionization produces a discharge relatively free of arcs up to the highest pressure tested, and the laser gives an energy density comparable to that with the 1-cm gap, but in a smaller beam of smaller divergence (determined by the aspect ratio of the gap). Fig. 1(c) shows the pressure dependence of the output, again for an atmospheric-pressure mixture of N_2 and He. Some laser output was observed with as much as 400 torr of N_2. Since the discharge does not appear arc dominated even for high nitrogen pressure, the decrease of laser power at high pressure can presumably be attributed to the decrease of E/p.

We believe on the basis of these measurements that it should be possible by using preionization together with higher voltages and shaping of the electrodes to achieve atmospheric or higher pressure operation with pure N_2 or possibly with a mixture of N_2 and a buffer gas suitable for collisional quenching of the lower levels [8].

ACKNOWLEDGMENT

The authors wish to thank J. G. Small, J. Goldhar, and J. S. Levine for a number of helpful discussions. They also wish to thank J. Taller and J. Devir for their technical assistance.

REFERENCES

[1] H. G. Heard, "Ultra-violet gas laser at room temperature," *Nature*, vol. 200, p. 667, 1963.

[2] a) E. T. Gerry, "Pulsed-molecular-nitrogen laser theory," *Appl. Phys. Lett.*, vol. 7, pp. 6–8, 1965.
b) A. W. Ali, "A study of the nitrogen laser power density and some design considerations," *Appl. Opt.*, vol. 8, pp. 993–996, 1969.

[3] (a) D. A. Leonard, "Saturation of the molecular nitrogen second positive laser transition," *Appl. Phys. Lett.*, vol. 7, pp. 4–6, 1965.
b) J. D. Shipman, Jr., "Traveling wave excitation of high power gas lasers," *Appl. Phys. Lett.*, vol. 10, pp. 3–4, 1967. (For reference to a number of other designs, see E. E. Bergmann and E. Eberhardt, "A short high-power TE nitrogen laser," *IEEE J. Quantum Electron.* (Corresp.), vol. QE-9, pp. 853–854, Aug. 1973.)

[4] I. N. Knyazev, V. A. Letokhov, and V. G. Movshev, "TEA N_2 UV laser with reduced spectra," *Opt. Commun.*, vol. 6, pp. 250–252, 1972.

[5] A. Javan and J. S. Levine, "The feasibility of producing laser plasmas via photoionization," *IEEE J. Quantum Electron.*, vol. QE-8, pp. 827–832, Nov. 1972.

[6] J. G. Small and R. Ashari, "A simple pulsed nitrogen 3371 A laser with a modified Blumlein excitation method," *Rev. Sci. Instrum.*, vol. 43, pp. 1205–1206, 1972.

[7] a) J. S. Levine and A. Javan, "Observation of laser oscillation in a 1-atmosphere CO_2-H_2-He laser pumped by an electrically heated plasma generated via photoionization," *Appl. Phys. Lett.*, vol. 22, pp. 55–57, 1973.
b) H. J. J. Seguin, J. Tulip, and D. McKen, "Enhancement of photoelectron density in TEA lasers using additives," *Appl. Phys. Lett.*, vol. 23, pp. 527–529, 1973.

[8] L. Y. Nelson, G. J. Mullaney, and S. R. Byron, "Superfluorescence in N_2 and H_2 electron-beam-stabilized discharges," *Appl. Phys. Lett.*, vol. 22, pp. 79–80, 1973.

Sealed multiatmosphere CO_2 TEA laser: Seed-gas compatible system using unheated oxide catalyst

R. B. Gibson and A. Javan

Department of Physics, Massachusetts Institute of Technology, Cambridge, Massachusetts 02139

K. Boyer

Los Alamos Scientific Laboratory, University of California, Los Alamos, New Mexico 87544
(Received 13 February 1978; accepted for publication 21 March 1978)

A sealed multiatmospheric CO_2 TEA laser is reported in which recombination of principle discharge products CO and O_2 is induced by recirculating the laser gas mixture through a room-temperature oxide catalyst bed. No special gas mixtures are required and the catalyst is compatible with at least some trialkylamine seed gases.

PACS numbers: 42.55.Dk, 42.60.By

Several researchers have reported sealed-off operation of cw CO_2 lasers. These systems have all used esoteric gas mixtures or have depended on catalytic action at electrodes or hot platinum wires or a combination thereof.[1–3] Recently, sealed TEA lasers have also been described, successful operation of which depends again on critical gas mixture.[4,5] Use of such lasers over a wide range of operating conditions or when optimization of characteristics other than lifetime is desired are difficult in practice. Willis *et al.*[5] has reported a TEA laser system in which a normal CO_2 laser mixture is pumped through a closed loop containing the laser, a heated (≥250 °C) bed of platinum catalyst, and a cooling coil to return the gas to room temperature. Such external control of gas chemistry permits greater flexibility in the laser mixture composition and operating conditions than previous schemes.

In this letter, we report a closed-cycle CO_2 TEA laser system similar to Willis but in which a room-temperature catalytic reaction is used to permit sealed-off operation over a wide range of pressures, mixtures, and operating conditions without the prodigious heating and cooling requirements inherent in precious metal catalysis. In addition, the system described has been found to be compatible with at least one "seed" gas of the trialkylamine family often used to aid photopreionization in double-discharge lasers.[7,8]

It is generally agreed that the primary impediment to sealed laser operation is dissociation of CO_2 in the discharge[1,9–11]:

$$CO_2 \xrightarrow{\text{DISCHARGE}} CO + \tfrac{1}{2}O_2.$$

In cw lasers, power output falls with the declining partial pressure of CO_2.[12] In TEA lasers, the build-up of O_2 in the cavity leads to arc formation after a few hundred shots and typically renders the laser useless after ~10^3 shots. The rate of O_2 formation may be as high as 0.1%/shot [3] but is typically an order of magnitude less.

The laser used in these experiments has an active volume of 15 ml, can be operated at any pressure up to 17 atm, and is normally pumped at ~200 J l^{-1} atm.$^{-1}$. Preionization is initiated by uv generated from discharging ~150 mJ into each of two segmented transmission lines parallel to the sustainer electrodes. To the normal laser mixture is added a small quantity of a seed gas which photoionizes easily in the weak uv discharge to produce the requisite initial electron density (≥ 10^8 cm^{-3}) needed to assure uniformity of the succeeding self-sustained discharge.

Among the most common seed gases used in the past have been the trialkylamines. A drawback of most of these is eventual decomposition and polymerization, solid and liquid products of which tend to coat window and electrode surfaces. This problem is avoided in this laser by using trimethylamine, $(CH_3)_3N$, as the seed gas at a concentration of ~0.1%. Though $(CH_3)_3N$ has the highest ionization potential (7.82 eV) and smallest uv absorption cross section of the trialkylamines, it appears stable in the discharge. No objectionable products have been observed in several hundred hours of flow-through operation involving 10^5–10^7 shots.

Recombination of the CO and O_2 produced in the discharge is encouraged in the sealed system by pumping the laser gas through a bed of hopcalite (60% MnO_2, 40% CuO, and trace quantities of other oxides), a common commercial catalyst long used in gas masks, mines, chemical plants, etc., to oxidize CO. (Other oxides and oxide combinations may also work.) While the mechanism by which this reaction occurs is more complicated than a simple oxidation-reduction process and is not thoroughly understood (see Brittan *et al.*[13] for a good discussion), it is known that the reaction rate is primarily dependent on CO partial pressure, p_{CO}.[14,15] A first-order approximation is adequate for present purposes:

$$-\frac{dp_{CO}}{dt} \propto p_{CO}.$$

Since O_2 adversely affects the discharge while even a few percent CO has no significant effect,[4] it is highly desirable to have more CO than O_2 in the system at any one time. Approximately 0.5% (not critical) CO is added to the laser gas mixture to ensure a high reaction rate. Without the extra CO, the reaction is so slow as to be ineffective in this application. Taylor *et al.*[2] first tried hopcalite in a cw laser but unsuccessfully, probably for this reason.

 0003-6951/78/3211-0726$00.50

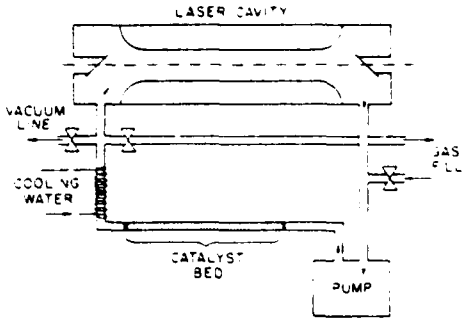

FIG. 1. Schematic of sealed CO_2 laser gas recirculation system. Total system volume is 1 l. Pump is metal bellows type with a positive displacement of 1 l sec^{-1}.

The sealed system is shown schematically in Fig. 1. The granular catalyst is loosely packed in a $\frac{1}{4}$-in.-o.d. copper tube and immobilized at each end by a fine copper screen and a loose glass wool dust trap. Another section of the tube is surrounded by a tap water coil. This adequately cools the gas, compensating for compression heating in the pump. The catalyst bed runs ~20 C above ambient temperature because of the latter effect but this slightly elevated temperature is unnecessary to proper catalyst operation.

To function properly, the catalyst must be reasonably dry. Should it become contaminated with water vapor, heating under vacuum restores its activity to original levels. This procedure is also routinely employed after any exposure to air. Ordinary commercial gases are used in our experiment without special precautions to ensure dryness.

The system described is operated from below atmospheric pressure to 5 atm (the limit of the pump) using the same gas mixtures as for flow-through operation except for the addition of CO as previously described. Mixtures vary widely according to application. Maximum repetition rate depends on amount of catalyst and pressure. A 1-Hz rate can be sustained at 1 atm with as little as 0.6 g of catalyst. Rates over 10 Hz have been sustained at 5 atm with 10 g in the loop. No deterioration in performance of the laser is noted after 10^5 shots and there is no evidence of reaction between catalyst and the seed gas as there is in hot platinum.

[1]W.J. Witteman, Appl. Phys. Lett. 11, 337 (1967).
[2]F.M. Taylor, A. Lombardo, and W.C. Eppers, Appl. Phys. Lett. 11, 180 (1967).
[3]A.L.S. Smith and P.G. Browne, J. Phys. D 7, 1652 (1974).
[4]D.S. Stark, P.H. Cross, and H. Foster, IEEE J. Quantum Electron. QE-11, 774 (1975).
[5]H. Shields, A.L.S. Smith, and B. Norris, J. Phys. D 9, 1587 (1976).
[6]C. Willis, R.A. Back, and J.G. Purdon, Appl. Phys. Lett. 31, 84 (1977).
[7]J.S. Levine and A. Javan, Appl. Phys. Lett. 22, 55 (1973).
[8]E. Morikawa, J. Appl. Phys. 48, 1229 (1977).
[9]J.M. Austin, A.L.S. Smith, and P.G. Browne, Phys. Lett. A 46, 427 (1974).
[10]A.L.S. Smith and J.M. Austin, J. Phys. D 7, 314 (1974).
[11]J. Freudenthal, J. Appl. Phys. 41, 2447 (1970).
[12]R.J. Carbone, IEEE J. Quantum Electron. QE-3, 373 (1967).
[13]M.I. Brittan, H. Bliss, and C.A. Walker, AIChE J. 16, 305 (1970).
[14]J.A. Almquist and N.C. Bray, J. Am. Chem. Soc. 45, 2305 (1923).
[15]W.E. Kuentzel, J. Am. Chem. Soc. 52, 437 (1930).

APPENDIX E

Thesis Abstracts of Students Supported by ONR Contract Funds

1) Francke - Study of Relaxation Processes in He_2 Using Pulsed Dye Laser Techniques
2) Fulghum - XeF Ground State Dissociation and Vibrational Equilibration
3) Goldhar - Charge Exchange Processes Involving Highly Stripped Ions Generated From Laser Produced Plasmas
4) Guerra - Infrared Spectroscopy Using a Tunable Laser
5) Hamadani - Investigation of Transient Coherent Optical Phenomena in Resonant Media
6) Herman - Laser-Initiated Chemical Reactions of NO_2 and Related Kinetic and Spectriscopic Studies
7) Kelly - Lineshapes of Narrow Doppler-Free Saturation Resonances and Observation of Anomalous Zeeman Splitting Arising from Rotational Magnetic Moment in $^1\Sigma CO_2$ and N_2O Molecules
8) Mattick - Determination of Velocity Dependence of Collision-Broadening Cross Sections Using Saturation Spectroscopy
9) Sheffield - Study of Vibrational and Rotational Relaxations of D_2O and the Related Spectroscopic Properties

STUDY OF RELAXATION PROCESSES IN He_2 USING PULSED DYE LASER TECHNIQUES

by

Ricardo Francke

Submitted to the Department of Physics in partial fulfillment of the requirements for the degree of Doctor of Philosophy.

ABSTRACT

The technique of laser-induced fluorescence using a pulsed dye laser has been applied to study processes in ground and excited triplet states of molecular helium. The technique is simple and generally applicable. In the present work it was used to study the formation and quenching of the ground triplet state $He_2(a^3\Sigma^+_u) = He_2^m$ and the relaxation processes of the $He_2(e^3\Pi_g)$.

In the experiment, a pulsed discharge in He is used to produce different excited species, some of which become He_2, which is then quenched by different mechanisms. In order to study the formation and decay of He_2, the electrical pulses were made purposely short, so the species of interest are created after the gas discharge. A nitrogen laser pumped dye laser was used to excite the $a^3\Sigma^+_u(v,N) \rightarrow e^3\Pi_g(v,N')$ λ=4650Å vibronic transitions of He in the afterglow of the gas discharge. The excitation was measured by monitoring the fluorescence emitted from the $e^3\Pi_g$ level of He_2. The detection system consisted of an optical system to collect light, and a monochromator followed by a cooled photomultiplier. The monochromator used as a filter is necessary to isolate the laser induced fluorescence from the noise of the discharge. The signal to noise ratio was further increased by using a gated integrator with an adjustable gate aperture time. A scanning device was incorporated into the system which varies the delay between the dye laser pulse and the helium discharge. In this way all the time evolution of He_2^m was obtained in one single scan. The high intensity and the short pulse of the dye laser (6 nsec FWHM) acted as a delta function excitation of the upper level. These features of this laser simplified the detection and data analysis of relaxation processes of the upper level being populated.

It was found that under the conditions used here, He_2^m is produced during the first 400 μsec of the afterglow from excited helium atoms. Also the formation rate of He_2^m coincides with the destruction rate of He^+ through transformation to He_2^+ and dielectronic recombination. This model also explains the variation of peak current during the glow with peak population of He_2^m. Furthermore, it also accounts for the time evolution of He_2^m. The rate of formation of He_2^m from He^+ was found to be (2.20±0.40) times the concentration of He^+. Of course the formation of He_2^m from He^+ could involve many other intermediate steps. In the experimental conditions of this work, other mechanisms that produce He_2^m are found to make very small contributions to the formation of He_2.

The main loss mechanism of He_2^m is diffusion to the walls. Another loss mechanism is electron quenching. The v=1 state was found to be quenched faster than v=0. The first one has a rate of $(9.00\pm2.90)\times10^{-9}$ cm^3/sec, while the v=0 has a rate of $(2.2\pm0.70)\times10^{-9}$ cm^3/sec. The dependence of this quenching rate on the vibrational quantum number was seen here for the first time.

It was also found that the lifetime "τ" of the $e^3\Pi_g$ state is given by $1/\tau = [37.22\pm8.5+(4.30\pm1.20)p]10^6 sec^{-1}$ where "p" is the pressure in torr. It was also found that a collision of an excited molecule with a helium atom could change the electronic state of the molecule. This collision transfer allowed me to measure the radiative lifetime of the $e^3\Pi_g$, $d^3\Sigma^+_u$, $f^3\Sigma^+_u$ and $f^3\Pi_u$ states as being 27±6, 53±5, 27±6, and 40±13 nsec, respectively. The collision transfer rate from the $e^3\Pi_g$ to the $d^3\Sigma^+_u$, $f^3\Pi_u$ and $f^3\Delta_u$ was measured as being $(6.70\pm1.39)\times10^6$, $(1.00\pm0.23)10^5$ and $(22.6\pm5.2)10^3$ $sec^{-1}torr^{-1}$ respectively. The collision transfer rate from the $e^3\Pi_g$ to the $f^3\Sigma^+_u$ was found to be extremely fast and such that at pressures above 3 torr the two levels were in thermal equilibrium. This rate was determined as being over 30×10^6 $sec^{-1}torr^{-1}$.

Ratios of Franck-Condon factors between the $e^3\Pi_g$ and $a^3\Sigma^+_u$ states were measured as $q_{00}/q_{01}=21.1$ and $q_{11}/q_{12}=9.84\pm0.39$,

Thesis Supervisors: Ali Javan and Michael S. Feld
Title: Professors of Physics

XeF GROUND STATE DISSOCIATION AND VIBRATIONAL EQUILIBRATION

by

STEPHEN FREDERICK FULGHUM JR.

Submitted to the Department of Physics on 4 October 1979
in partial fulfillment of the requirements
for the Degree of Doctor of Philosophy

ABSTRACT

The XeF molecule is unusual among the rare gas monohalides in that it has a bound ground electronic state. The potential well is about 1200 cm^{-1} deep, highly anharmonic and supports about 10 vibrational levels. The molecule is rapidly dissociated by collisional processes. This thesis reports the determination of the dissociation and vibrational equilibration rates of XeF in rare gas buffers.

Two types of experiments have been performed. The first uses an absorption technique to measure the overall dissociation rate of XeF formed in a Xe, F_2, and He discharge at pressures of from about 100 to 1000 Torr. The second experiment uses a laser induced fluorescence technique to measure overall dissociation rates of XeF formed by the photodissociation of XeF_2 vapor by an ArF laser pulse in rare gas buffers at pressures of from 0 to 100 Torr. The rates measured by the two experiments are essentially identical at $9.9\ (\pm 2.5)\times 10^3$ sec^{-1} $Torr^{-1}$ for a He buffer. The second experiment also allows the determination of a characteristic vibrational equilibration rate. The XeF is rapidly produced in a nonthermal distribution, primarily in high lying vibrational states, and the approach of the $v''=0$ and 1 levels toward a quasiequilibrium is monitored.

These rates are characteristic of the vibrational manifold as a whole. Microscopic VT rates and individual direct dissociation rates out of each level are determined by fitting a 10-level model to the exerimental data. The VT

rates are modeled using a prior rate and a linear surprisal given by the information theoretic approach of Levine and co-workers. The dissociation rates are modeled with a variation of the Arrhenius equation which includes a surprisal-like parameter in the pre-exponential term. This allows for variations in the dissociation rate which depend specifically on the vibrational level in question.

This model is used to simulate an XeF laser in order to study the effects of the experimentally derived rates on laser efficiency and the competition between the various laser transitions. It is found that the finite lifetime of the ground state decreases the efficiency of an atmospheric XeF laser by about 30% in the quasi-CW limit.

Thesis jointly supervised by:

Ali Javan, Francis Wright Davis Professor of Physics

Michael S. Feld, Professor of Physics
Director, Spectroscopy Laboratory

CHARGE EXCHANGE PROCESSES INVOLVING HIGHLY STRIPPED IONS GENERATED FROM LASER PRODUCED PLASMAS

by

JULIUS GOLDHAR

Submitted to the Department of Physics on January 14, 1976, in partial fulfillment of the Requirements for the degree of Doctor of Philosophy.

ABSTRACT

Experimental study of charge transfer between highly stripped ions and noble gas atoms was conducted. The ions were generated from laser produced plasmas. One and two electron transfer to C^{+3}, C^{+4}, and C^{+5} was observed. Aluminum and silicon ions were also generated and charge exchange cross-sections for them were measured. The hot plasma was generated by focusing the output of the CO_2 oscillator-amplifier laser system. 100MW pulses of ten nanosecond duration was used.

Large cross-sections observed for some collisional reactions indicate that resonant two-electron transfer processes play an important role in charge transfer.

Thesis Supervisor: Ali Javan
Title: Professor of Physics

INFRARED SPECTROSCOPY USING A TUNABLE LASER

by

Michael Guerra

Submitted to the Department of Physics on February 11, 1976
in partial fulfillment of the requirements for
the degree of Doctor of Philosophy

ABSTRACT

A low field permanent magnet spin-flip Raman laser was designed and constructed. Using tapered pole pieces and a moveable platform, it was possible to vary the field of the permanent magnet. The frequency of the spin-flip laser was stabilized by locking it to a passive Fabry-Perot cavity. This system was utilized to do high resolution multi-photon spectroscopy in nitrix oxide.

A novel use was made of a waveguide with flared ends to provide high intensity fields and eliminate diffrations limiting effects for the two photon work. A number of materials with different configurations were tested and the transmission results are given. It was found that a .6mm bore and 60cm long Pyrex capillary with flared conical ends gave 60% transmission at 5.3 microns.

Some basic theory of two-photon Doppler free spectroscopy is discussed and its relation to laser induced line narrowing effects is pointed out.

A narrow Doppler free two-photon resonance is observed for the J=12.5 v=0 → J=14.5 v=2 transition in NO. The width of the resonance being 12MHz (FWHM) as compared to the Doppler width of 128 MHz. Its magnitude is shown to be in good agreement with that predicted by theory.

In addition, a series of stepwise excitations are used to study the position and Λ-splitting of several different J lines in the first hot band of NO. From the measurements of the absolute frequencies of these lines, it is found that the band edge of the 2→0 transition in NO lies at 3724.100±.003 cm^{-1}. This represents a shift downward of 540 MHz from the previous reported value. From this, the first anharmonic vibrational constant is found to be $\omega_e\chi_e$ = 13.964±.015 cm^{-1}.

The Λ-doubling values are used to measure the vibrational dependence of the p_Λ constant and its value is found to be given by $p_\Lambda = 176.15-1.358\pm.53$ MHz. This is the first experimental measurement of a vibrational dependence for the Λ-doubling constants in any system. It is shown that this value is in good agreement with a very simple approximation proposed by Van Vleck.

Thesis Supervisor: Ali Javan
Title: Professor of Physics

INVESTIGATION OF TRANSIENT COHERENT OPTICAL PHENOMENA IN RESONANT MEDIA

by

SIAVOSH MOSHFEGH HAMADANI

Submitted to the Department of Physics on January 15, 1976

in partial fulfillment of the requirements for the

degree of Doctor of Philosophy.

ABSTRACT

Transient coherent phenomena are investigated in this thesis by means of studying

a) The evolution of the envelope of short duration (2-40nsec) N_2O laser pulses in resonant NH_3 absorber for a variable number of absorption lengths ($\alpha L \lesssim 14$). Zero degree pulses ($\int_{-\infty}^{+\infty} \varepsilon(z,t)dt=0$) are observed to propagate with enhanced transmission for both short-duration low intensity pulses and longer pulses of intensity sufficient to allow observation of optical nutation effects. The reshaping of pulses which contain a rapid amplitude or phase variation is observed to result in pulses of subnanosecond duration. A rapid phase reversal gives rise to amplification for times comparable to the transverse relaxation time.

b) The evolution of the envelope of short-duration (2-40nsec) CO_2 laser pulses in a low pressure ($\sim$5 Torr) CO_2 amplifier in the linear regime for a variable number of gain lengths ($\alpha L \lesssim 7$). Single pulses grow considerably in duration as well as amplitude in agreement with theoretical considerations. Analysis of the observed pulse evolution is used to obtain experimental values for the transverse relaxation parameter T_2 and the number of gain lengths αL in agreement with values obtained by other methods. Zero degree pulses are observed to terminate much of the long tail which occurs in single pulse amplification. Off-resonant amplification of short duration pulses is shown to lead to dramatic changes in the zero-degree pulse evolution. Numerical calculations relating to the use of these techniques in the nonlinear regime for high pressure CO_2 amplifiers are also presented.

c) The properties of population inversion by optical Adiabatic Rapid Passage (ARP) using laser saturation spectroscopy techniques. In these investigations, a direct attempt to measure T_1 in the time domain for an infrared transition in NH_3 is undertaken. The population change produced by sweeping the frequency of a strong saturating N_2O laser field through the center of a Doppler-broadened absorption line is probed by a weak counterpropagating field as in a Lamb-dip experiment. When the ARP conditions are satisfied, inversion of population is detected as amplification of the probe wave near the line center. As the inverted population relaxes to equilibrium, the amplification decays back to the unsaturated absorption with a time constant given by T_1. The pressure dependence of this decay below 40 mTorr is measured to be $T_1P=24.3(\mu sec \cdot mTorr)$ indicating that $T_1 \simeq 3.6\ T_2$. The results are discussed in terms of molecular dipole-dipole interactions, responsible in NH_3 for the collision-induced decay of the polarization as well as that of the population inversion.

Thesis Supervisor: Ali Javan

Title : Professor of Physics

LASER-INITIATED CHEMICAL REACTIONS OF NO_2 AND RELATED KINETIC AND SPECTROSCOPIC STUDIES

by

IRVING PHILIP HERMAN

Submitted to the Department of Physics in partial fulfillment of the requirements for the Degree of Doctor of Philosophy in April 1977.

ABSTRACT

Experiments are described in which electronically excited NO_2 is observed to react with CO, to form NO and CO_2, at a rate many orders of magnitude faster than the associated thermal reaction. In addition, an exploratory spectroscopic analysis of NO_2 using infrared-optical double resonance (IODR) is reported.

In the reaction studies NO_2 is excited to the $^2B_2$ electronic state by either a cw argon-ion laser or a cw Rhodamine 6G dye laser. The room temperature-gas phase mixture ($\sim$ few torr) then reacts and the distilled CO_2 product concentration is subsequently measured by laser-induced fluorescence with a CO_2 laser.

The technique of CO_2 laser-induced fluorescence (with 10.6 μ excitation and 4.3 μ fluorescence) is described in detail. It is discovered that fluorescence from the CO_2 product ($\sim$ m torr) increases by an order of magnitude with the addition of argon at 1 torr. This buffer prevents rapid CO_2 diffusion to the walls and provides a linear calibration of fluorescence intensity versus CO_2 concentration.

Using this technique, and previously measured relaxation rates, the determined reaction rate constant with 4880 Å excitation is $k_R = 3.2 \pm 1.2 \times 10^{-15}$ cc/molecule-sec. The observed dependences on laser intensity and reactant concentration are in agreement with a proposed mechanism in which: $NO_2^* + CO \rightarrow NO + CO_2$ is the main step. Other possible mechanisms are found to disagree with experimental evidence.

k_R is found to smoothly increase by a factor of 10 as the exciting wavelength is decreased from 6125 Å to 4579 Å. This behavior is compared to a model in which RRK theory predicts reactivity and a step-ladder model describes relaxation. The observed activation energy, $\sim$ 1.7 ev, appears to be 0.4 ev higher than the thermal energy barrier.

In the exploratory excited-state IODR study, resonances are unexpectedly observed at each pair of argon-ion laser (multimode) and CO_2 laser wavelength employed. Detection is by infrared laser-modulated visible fluorescence. This fluorescence is found to be partially blue-shifted from the exciting wavelength. Narrow 1 GHz resonances are observed as a function of the visible laser single mode frequency (at fixed infrared wavelength) amidst a non-zero background.

The CO_2 laser is also used as a spatial probe of NO_2* diffusion. This study indicates that the NO_2* states involved in IODR have radiative lifetimes ($\sim$ 0.6 μ sec) much shorter than "bulk" one photon fluorescence ($\sim$ 75 μ sec).

Most wavelength pairs lead to an increase in fluorescence. However, the 4880 Å - R(12) 10.3 μ pair instead leads to a decrease, thereby suggesting that the hitherto unobserved $^2A_2$ electronic state is being excited.

These investigations indicate that the infrared transition in IODR occurs from a level closely collision-coupled to the directly laser-excited state.

Thesis Supervisor: Ali Javan
Title: Professor of Physics

LINESHAPES OF NARROW DOPPLER-FREE SATURATION RESONANCES AND OBSERVATION OF ANOMALOUS ZEEMAN SPLITTING ARISING FROM ROTATIONAL MAGNETIC MOMENT IN $^1\Sigma$ CO_2 AND N_2O MOLECULES

by

Michael James Kelly

Submitted to the Department of Physics on February 20, 1976 in partial fulfillment of the requirements for the degree of Doctor of Philosophy.

ABSTRACT

Several experiments are described which extend the possibilities of performing high resolution nonlinear laser spectroscopy by utilizing Doppler-free standing wave saturation resonances (SWSR). Theoretical lineshape calculations are performed on two and three level systems. The resulting lineshapes are then fitted to experimental data.

The lineshape of a three level system with two closely spaced levels interacting with a weakly saturating plane standing wave laser field is derived. It is shown that this lineshape can be considerably simplified before it is compared to the experimental data.

Using the rate equation approach, the lineshape of a two level system interacting with a strongly saturating standing wave field is calculated. This calculation includes a derivation of the 30% theoretical maximum depth of the saturation resonance observed in fluorescence. This lineshape is averaged over a Gaussian intensity distribution and yields a closed form solution. This solution permits the derivation of an expression for the half-width at half-maximum (HWHM) which is not limited to third- or fourth-order perturbation theory. Hence, this expression contains the effect saturation broadening. The intensity averaged line...

the interesting property that it predicts anomalous line narrowing at low pressure.

The design features of a highly stable 4-rod laser, useful for precision spectroscopy, is presented. The laser structure can be operated as either a CO_2 or N_2O laser. It oscillates on several hundred transitions in the 9-,10-, and 11-micron bands. Also, the development of a large area (2 cm x 2 cm) liquid helium cooled Cu:Ge detector with a cold filter which has a S/N comparable to InSb is presented.

A study of feedback effects on CO_2/N_2O laser stability demonstrated that feedback can effect the laser cavity power by as much as ±10% without producing any measurable frequency pulling effects. Several techniques of feedback isolation were investigated. The technique of misaligning the standing wave mirror was shown to produce a 35 kHz per mrad broadening of the HWHM of a saturation resonance.

Collision- and power-broadening measurements of CO_2 and N_2O fluorescence saturation resonances in the 0 to 70 mTorr region are presented. The slope of the collision-broadening data in this region varies from 6 to 16 kHz/mTorr. The data indicates that the transit time is not responsible for the anomalous line narrowing observed at low pressures. A fivefold reduction in the linewidth of these resonances is achieved. The experimental results demonstrate that there are no barriers which would prevent the use of these narrow Doppler-free fluorescence resonances in future clock applications.

The observation of Zeeman splitting of excited vibrational states of CO_2 ($10^00,02^00,00^01$) and N_2O ($10^00,00^01$) using the SWSR technique is reported. Observation of the small Zeeman splitting (~60kHz/kG) in these $^1\Sigma$ molecules is made possible by the narrow linewidth obtained by this technique. The existence of hundreds of lasing transitions in CO_2 and N_2O enables investigation of molecular g-factors across the whole vibrational band. The anomalous Zeeman effect resulting from the small difference in the g-factors of the two levels (~1-2%), due primarily to molecular vibration, produces a large difference in the observed lineshapes for P- and R-branch transitions. Experiments with linearly and circularly polarized light determine g and Δg to be: CO_2, 10-micron band, $g=-0.053\pm0.003$, $\Delta g=0.00100\pm0.00006$; CO_2, 9-micron band, $g=-0.052\pm0.003$, $\Delta g=0.00100\pm0.00006$; N_2O, 10-micron band, $g=-0.077\pm0.008$, $\Delta g=0.00077\pm0.00008$ where the magnitude of the lower level g-factor is greater than the magnitude of the upper level g-factor.

Thesis Supervisor: Ali Javan
Title: Professor of Physics

DETERMINATION OF VELOCITY DEPENDENCE OF COLLISION-BROADENING CROSS SECTIONS USING SATURATION SPECTROSCOPY

by

Arthur Thomas Mattick

Submitted to the Department of Physics on August 25, 1975 in partial fulfillment of the requirements for the degree of Doctor of Philosophy.

ABSTRACT

The technique of laser saturation spectroscopy was employed to observe narrow saturation resonances in NH_3 gas at room temperature due to molecules having prescribed velocity components v_z along the laser propagation direction. Velocity selection was achieved by using two counterpropagating fields having different frequencies to saturate and probe the gas, and in this way it was possible to measure the velocity dependence of collision broadening of the ν_2[asQ(8,7)] transition over a range of mean NH_3 velocities of 0.8 to 2.1 times the average thermal velocity, or a corresponding temperature range of 200° to 1200° K.

An acoustooptic modulator was utilized in the experiment for frequency-shifting the output of an N_2O laser to generate saturating and probe fields having different frequencies. Ammonia self-broadening and xenon broadening was measured at pressures below 100 mTorr for molecules with $v_z=0$ (Lamb dip) and for five non-zero velocities. The self-broadening coefficient exhibited a small velocity dependence consistent with that expected for a dipole-dipole intermolecular force. The increase in the linewidth of about 14% between $v_z=0$ and $v_z=1.2\times10^5$ cm/sec could be attributed to additional shorter range forces.

Xenon broadening showed an increase in the linewidth of more than 50% over the same range of selected velocities. The measured broadening coefficient of 7.2 MHz/Torr for xenon broadening was 5 times larger than predicted by considering only phase-changing and inelastic collisions. Both the observed

velocity dependence and the large broadening coefficient were accounted for in terms of velocity-changing collisions.

A theoretical investigation was made of the influence of level degeneracy and crossed polarizations for the saturating and probe fields on the saturation resonance lineshape. The expressions obtained for the lineshape in the limit of small saturating field intensities (rate equation approximation) were used to determine the T_1 relaxation rates for self-broadening and xenon broadening from the measured linewidths and the heights of the saturation resonances.

The saturated absorption method was also used to observe the previously unresolved hyperfine structure of the ν_2[asQ(8,7)] transition in NH_3. By comparing the splitting of the hyperfine components with that observed for the microwave inversion transition in NH_3, the hyperfine quadrupole interaction was found to be 17±10% stronger in the excited ν_2 state than in the ground state.

Thesis Supervisor: Norman A. Kurnit

Title: Assistant Professor of Physics

STUDY OF VIBRATIONAL AND ROTATIONAL RELAXATIONS OF D_2O AND THE RELATED SPECTROSCOPIC PROPERTIES

by

RICHARD LEE SHEFFIELD

Submitted to the Department of Physics on August 4, 1978 in partial fulfillment of the requirements for the Degree of Doctor of Philosophy.

ABSTRACT

This thesis is a study of the vibrational and rotational relaxations of D_2O and the spectroscopy and optical pumping of the ν_2 band of D_2O. The relaxation studies are the first room-temperature measurements of either vibrational or rotational relaxation of D_2O. Among the spectroscopic results are precise frequency measurement, a value for the dipole moment matrix element, and measurement of the collisional broadening coefficient.

The relaxation measurements were performed with a pulsed CO_2 laser resonantly exciting one of the rotational-vibrational transitions of the 000-010 absorption band; the resultant changes of the rotational-vibrational level populations and the time evolution of these changes back to the equilibrium state were observed by means of a low power CW CO_2 laser probing a number of resonant transitions in 000-010 and 010-020 absorption bands. This procedure yielded the deactivation rates of the D_2O (010) vibrational state due to self-collisions and to collisions with a number of buffer gases. The self-deactivation is measured to be 1.0 μs-Torr and the buffer gas deactivation ranges from 1.2 μs-Torr for H_2O to 600 μs-Torr for O_2.

In addition, there is an observation of an exceptionally long rotational relaxation time in a high-lying rotational level of the D_2O (010) state when the probe is set to the 9R36 CO_2 laser line. The measured thermalization rates of this level due to self-relaxation and collisions with buffer gases are found to range from a value of 100 μs-Torr for collisions with Argon to 0.4 μs-Torr for self-relaxation. The thermalization rate for a low-lying D_2O (000) rotational level is also reported and found to be in the typical range of 0.035 μs-Torr.

For the above measurements, it is necessary to have spectroscopic information on the ν_2 band of D_2O. To this end, a number of absorption resonances in the ν_2 band of D_2O in near coincidence with CO_2 laser lines are detected and their spectroscopic assignments identified.

Acousto-optic modulation is used to tune the 9 μm R(22) line of the CO_2 laser into coincidence with the $000,5_{3,3}$-$010,4_{2,2}$ D_2O transition (the center frequency of this line is measured to be 1079.8628 cm^{-1}; the line width (HWHM) due to collisional broadening is 15 MHz-$Torr^{-1}$).

Optical pumping is used to induce strong laser emission at new submillimeter wavelengths providing new laser sources at far-infrared frequencies and confirm the transition assignments.

Thesis Supervisor: ALI JAVAN

Title: Professor of Physics


DAT
FILM